



Effects of the First-Order Chiral Phase Transition in Relativistic Heavy-Ion Collisions

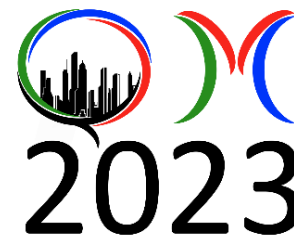
KaiJia Sun

kjsun@fudan.edu

Institute of Modern Physics, Fudan University, China



復旦大學
FUDAN UNIVERSITY



Quark Matter 2023
Houston, Texas
Sep 6 (2023)

Outline

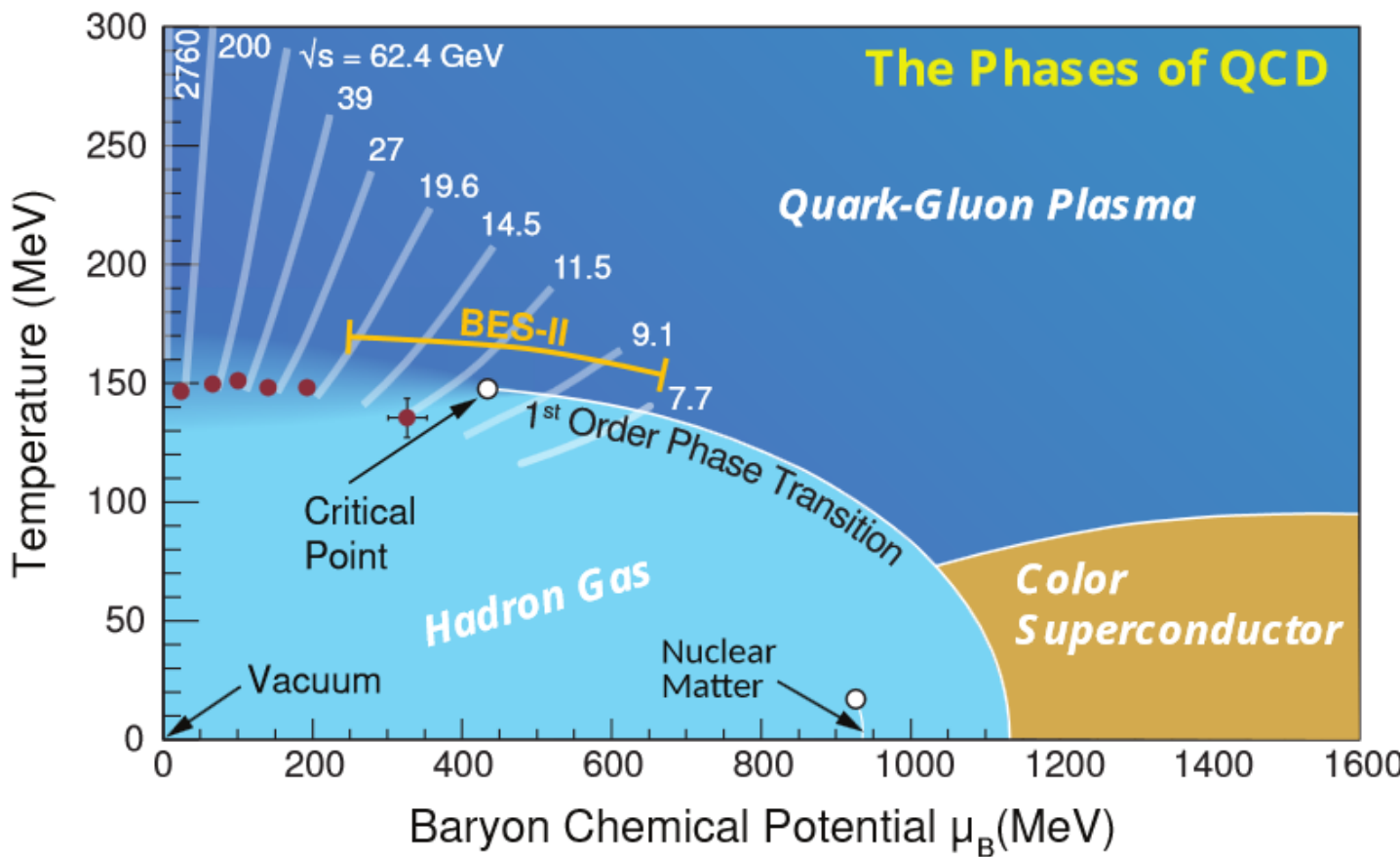
1. Motivation
2. Transport approach to the first-order chiral phase transition
3. Spinodal enhancement of $N_t N_p / N_d^2$
4. The triton ‘puzzle’ and its solution (RHIC and LHC)
5. Summary

Refs.: K. J. Sun, W. H. Zhou, L. W. Chen, C. M. Ko, and F. Li, R. Wang, and J. Xu, arXiv:2205.11010(2022)
K. J. Sun, R. Wang, C. M. Ko, Y. G. Ma, and C. Shen, 2207.12532(2022)

1. Motivation

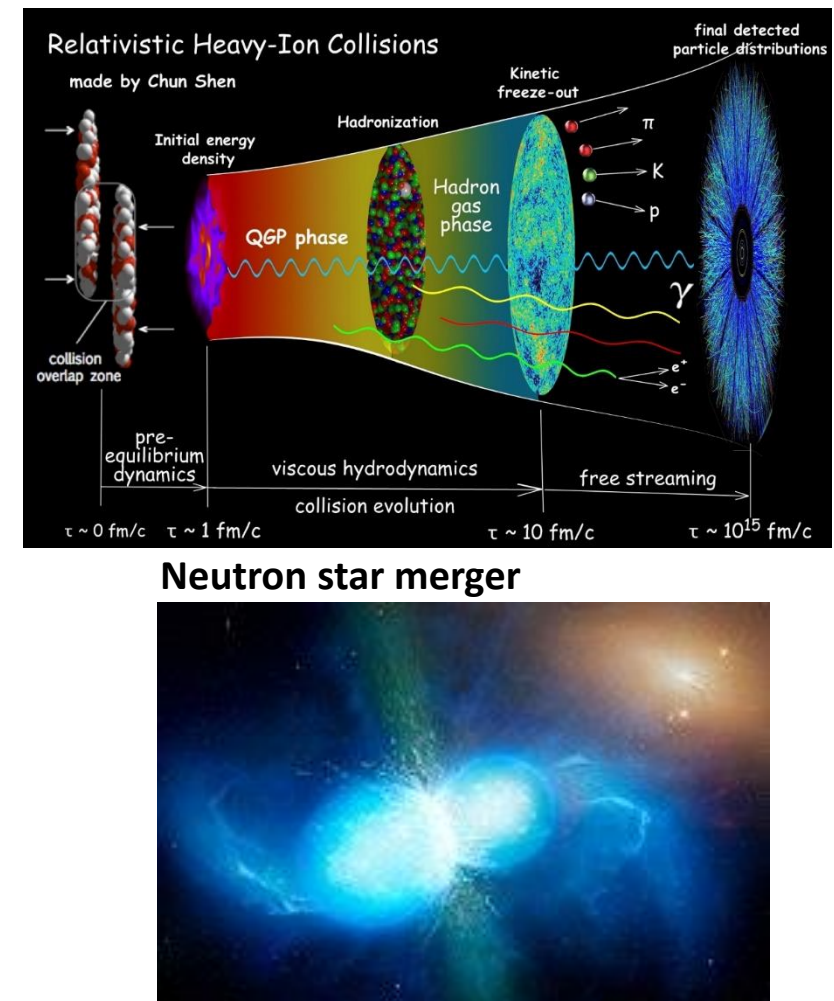
Hunt for the QCD critical point

(1)



Critical Point: long-range correlation

First-order Phase Transition: Spinodal instability



From Wiki.

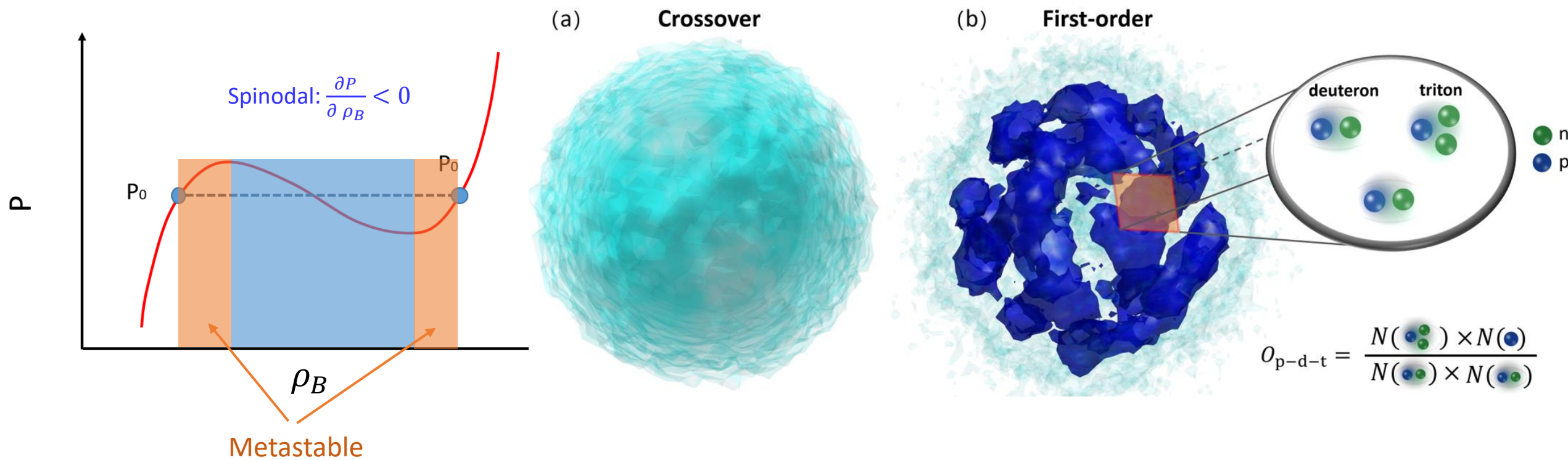
X. Luo and N. Xu, Nucl. Sci. Tech. 28, 112 (2017) A. Bzdak et al., Phys. Rept. 853, 1 (2020);

W. J. Fu, J. M. Pawłowski, F. Renneke, Phys. Rev. D101, 054032 (2020); LIGO & VIRGO, Phys. Rev. Lett. 119, 161101 (2017)

Idea: Probing QCD phase transition with light nuclei(2)

C. M. Ko, NST 34, 80 (2023).

[Poster by Koichi Murase]

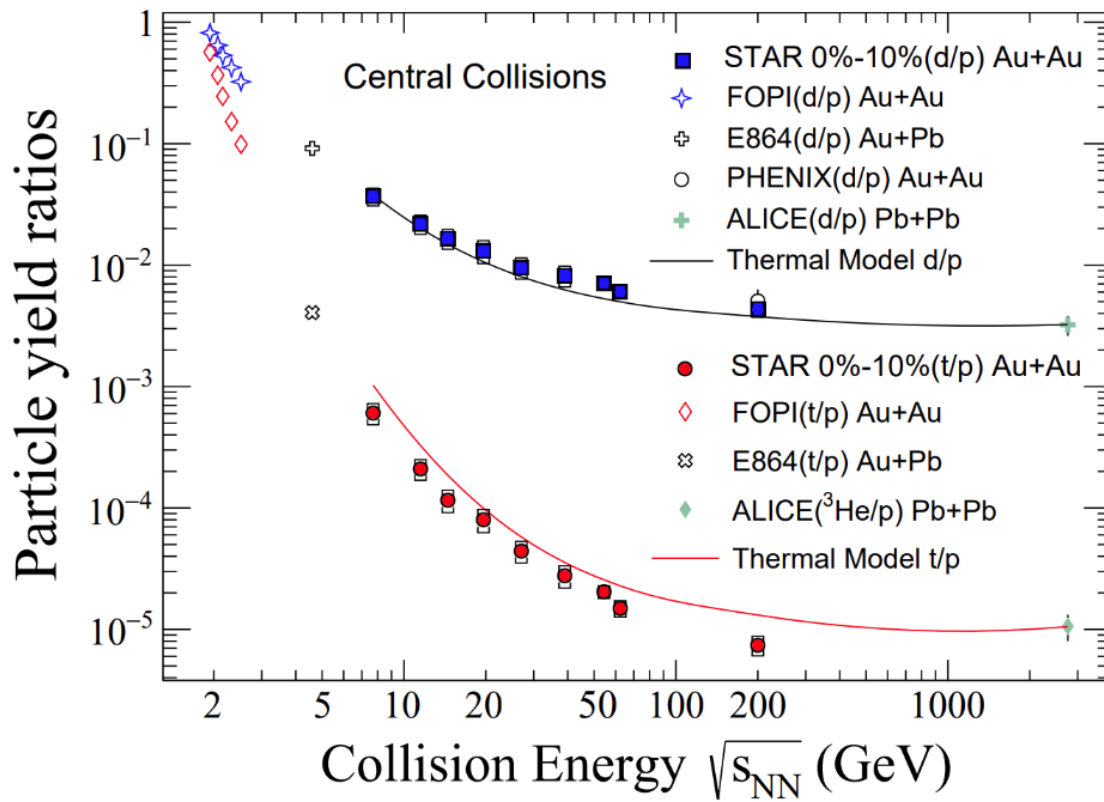


$$\text{Large density fluctuations lead to enhancements of } N_t N_p / N_d^2 \approx \frac{1}{2\sqrt{3}} \left[1 + \Delta\rho_n + \frac{\lambda}{\sigma} G\left(\frac{\xi}{\sigma}\right) \right]$$

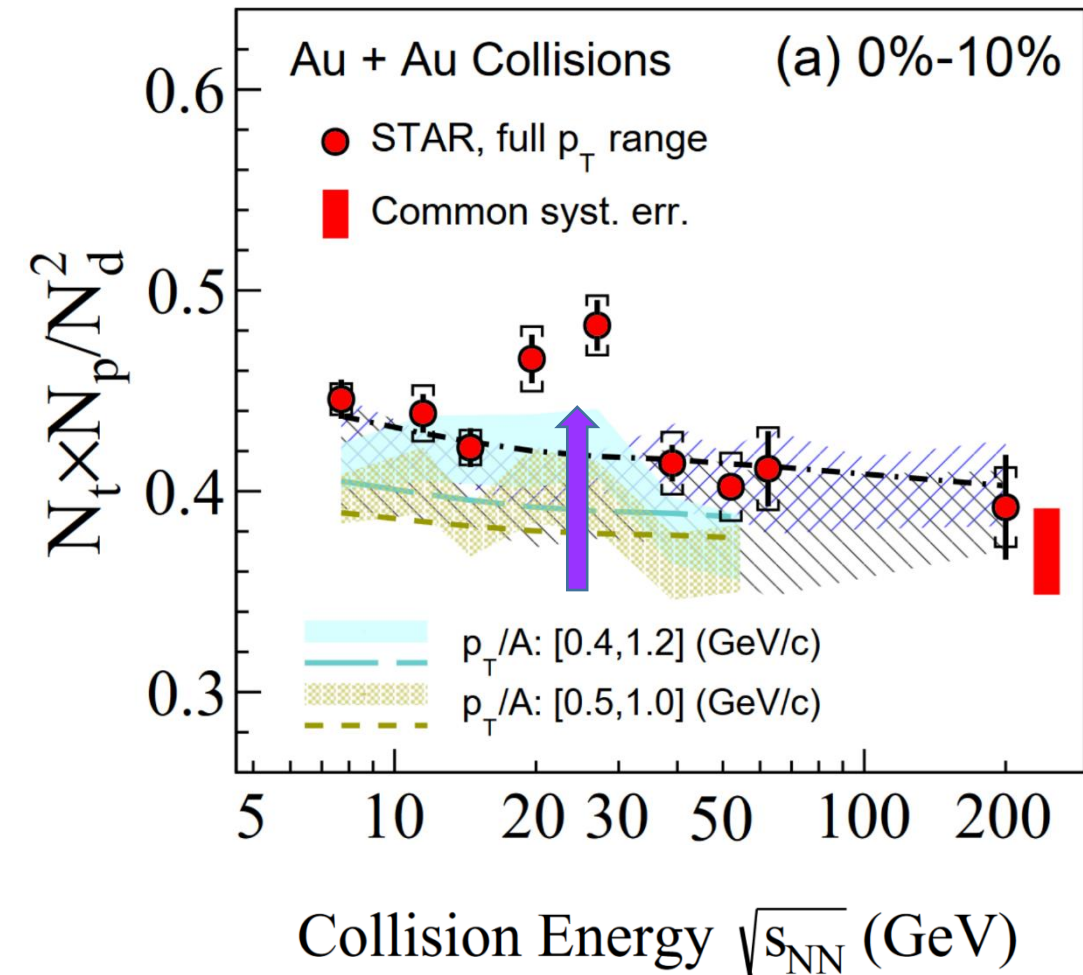
Recent STAR measurements

(3)

STAR: PRL130, 202302 (2023)



[Poster by Yixuan Jin for STAR]



2. Transport approach to the first-order chiral phase transition

Equation of state (extended NJL model)

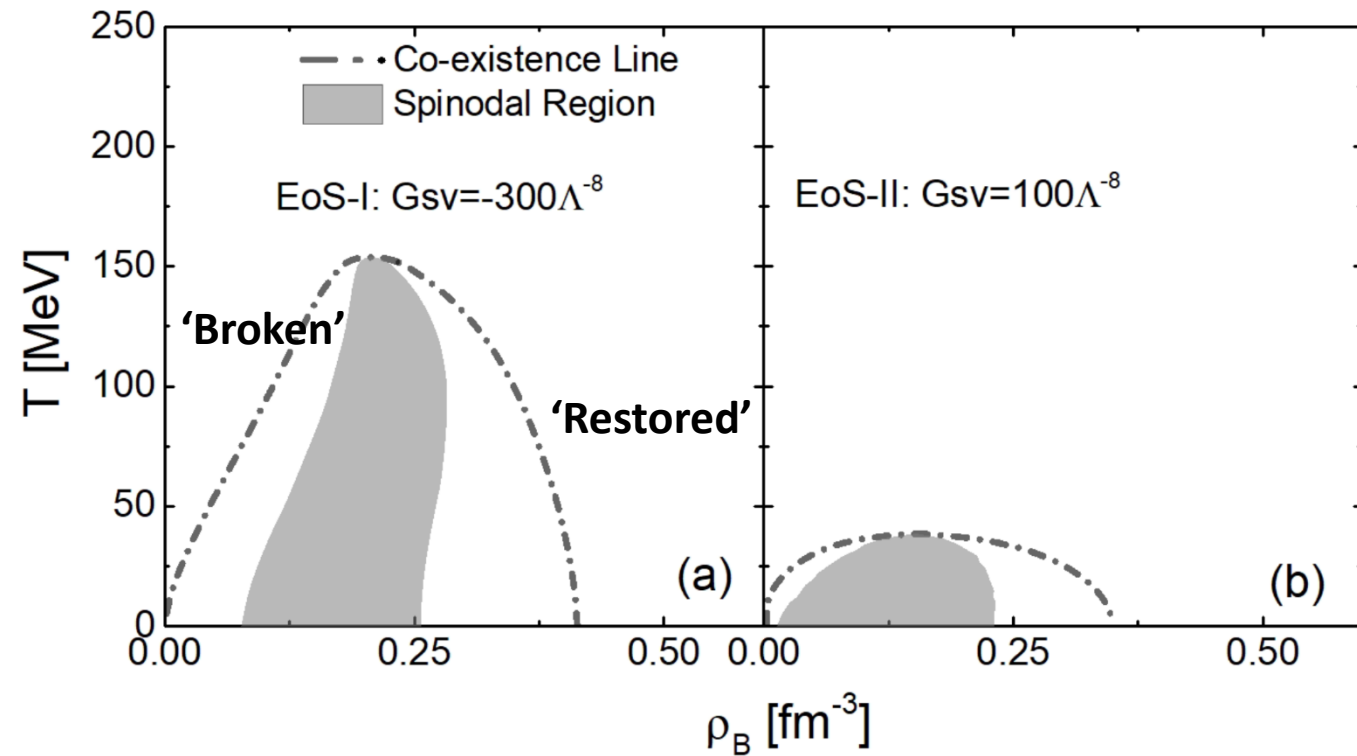
(4)

The eNJL provides a flexible equation of state (EoS) . The critical temperature can be easily changed by varying the strength of the scalar-vector interaction without affecting the vacuum properties.

Lagrangian density for an extended Nambu-Jona-Lasinio (eNJL) model

$$\begin{aligned} \mathcal{L} = & \bar{\psi}(i\gamma^\mu\partial_\mu - \hat{m})\psi + G_S \sum_{a=0}^3 [(\bar{\psi}\lambda^a\psi)^2 + (\bar{\psi}i\gamma_5\lambda^a\psi)^2] \\ & - K\{\det[\bar{\psi}(1 + \gamma_5)\psi] + \det[\bar{\psi}(1 - \gamma_5)\psi]\} \\ & + G_{SV} \left\{ \sum_{a=1}^3 [(\bar{\psi}\lambda^a\psi)^2 + (\bar{\psi}i\gamma_5\lambda^a\psi)^2] \right\} \\ & \times \left\{ \sum_{a=1}^3 [(\bar{\psi}\gamma^\mu\lambda^a\psi)^2 + (\bar{\psi}\gamma_5\gamma^\mu\lambda^a\psi)^2] \right\}, \end{aligned}$$

Λ [MeV]	602.3	$M_{u,d}$ [MeV]	367.7
$G\Lambda^2$	1.835	M_s [MeV]	549.5
$K\Lambda^5$	12.36	$(\langle \bar{u}u \rangle)^{1/3}$ [MeV]	-241.9
$m_{u,d}$ [MeV]	5.5	$(\langle \bar{s}s \rangle)^{1/3}$ [MeV]	-257.7
m_s [MeV]	140.7		



M. Buballa, Phys. Rept. 407, 205 (2005)

K. J. Sun, C. M. Ko, S. Cao, and F. Li., Phys. Rev. D 103, 014006 (2021)

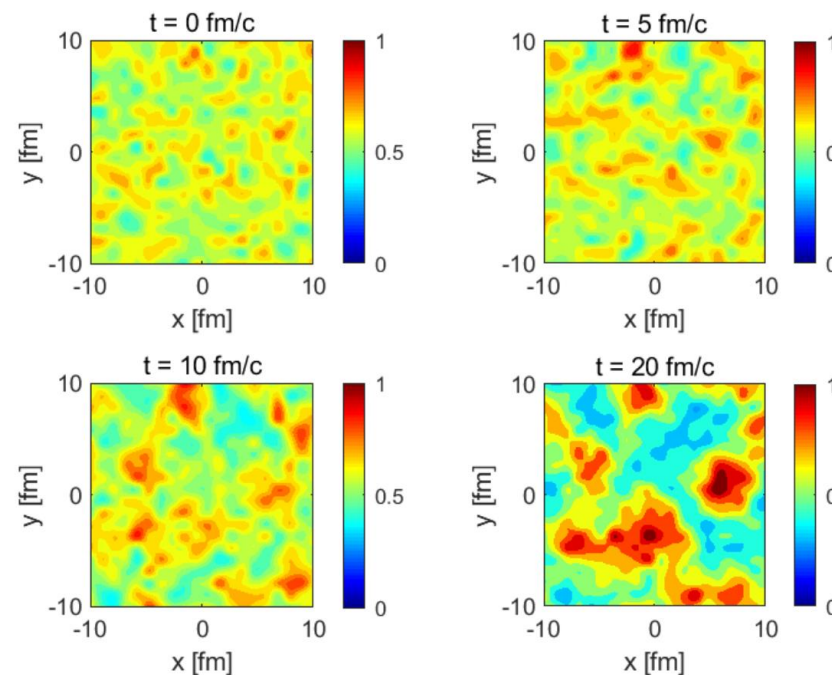
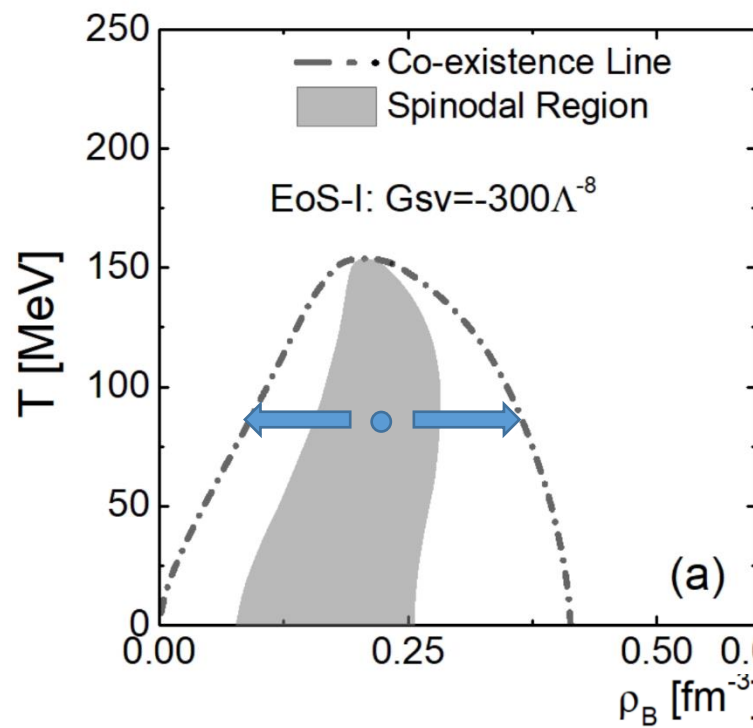
Box simulation

(5)

Effective mass:

$$\begin{aligned} M_u &= m_u - 4G_S\phi_u + 2K\phi_d\phi_s \\ &\quad - 2G_{SV}(\rho_u + \rho_d)^2(\phi_u + \phi_d), \\ M_d &= m_d - 4G_S\phi_d + 2K\phi_u\phi_s \\ &\quad - 2G_{SV}(\rho_u + \rho_d)^2(\phi_u + \phi_d), \\ M_s &= m_s - 4G_S\phi_s + 2K\phi_u\phi_d \end{aligned}$$

$$\begin{aligned} \phi_i &= -2N_c \int_0^\Lambda \frac{d^3 p}{(2\pi\hbar)^3} \frac{M_i}{E_i} (1 - f_i - \bar{f}_i) \\ \rho_i &= 2N_c \int_0^\Lambda \frac{d^3 p}{(2\pi\hbar)^3} (f_i - \bar{f}_i) \end{aligned}$$

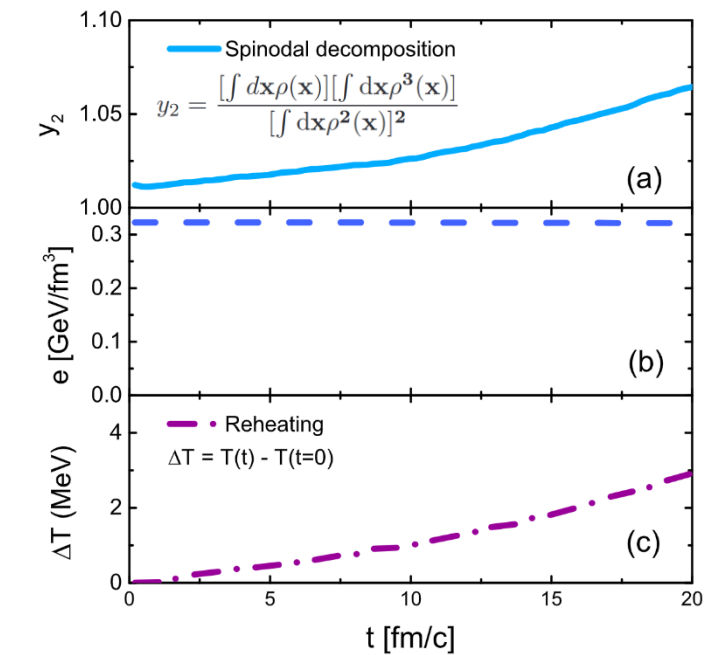


[Spinodal instability: see talk by Roman Poberezhnyuk]

Test-particle method: J. Xu, arXiv:1904.00131 (2019)

$$\begin{aligned} \frac{dr}{dt} &= \mathbf{v}, \\ \frac{d\mathbf{p}}{dt} &= -\frac{M}{E^*} \nabla_r M \pm \mathbf{E} \pm \mathbf{v} \times \mathbf{B} \end{aligned}$$

Strong EM fields

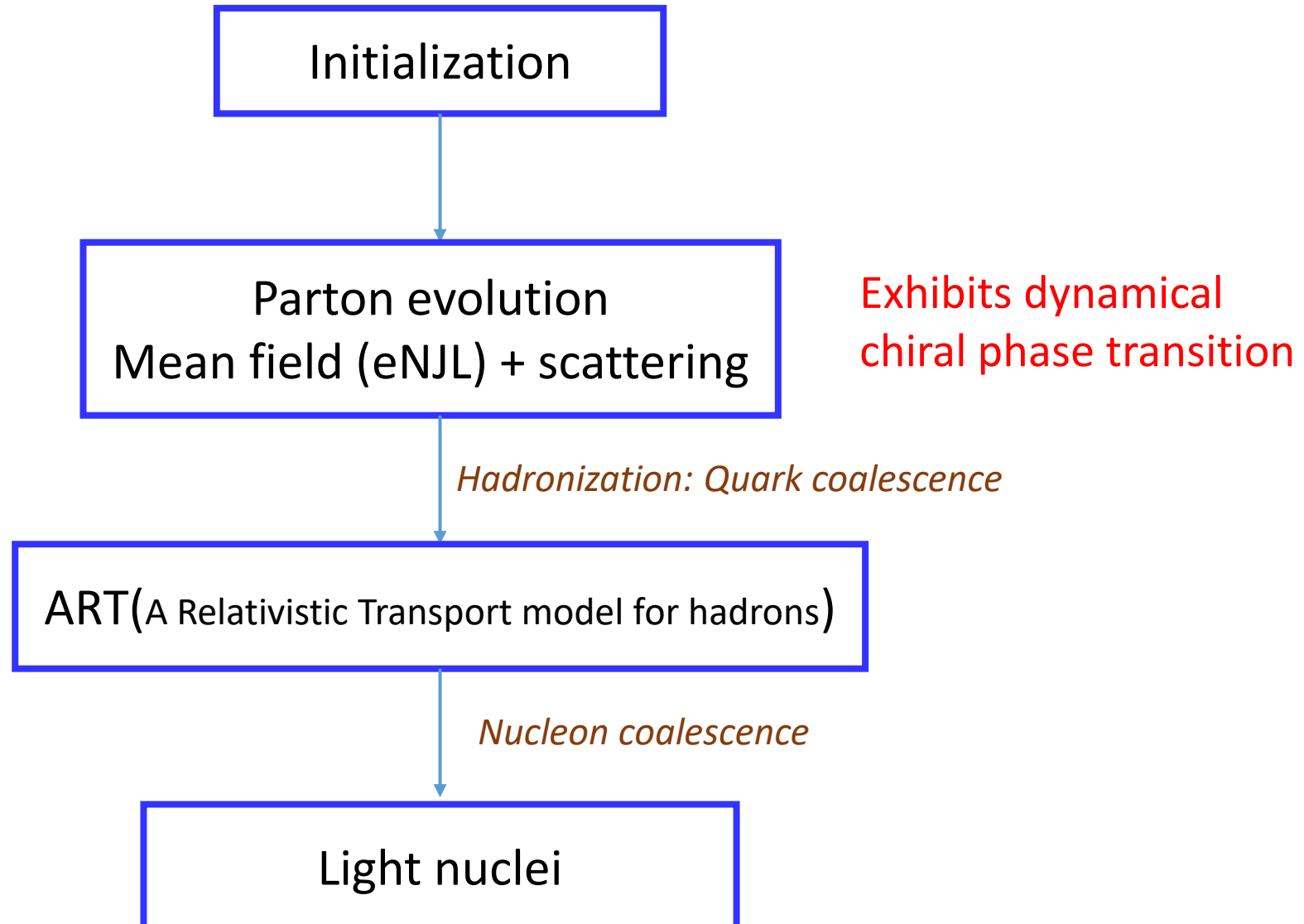


Small irregularities will grow exponentially and soon the evolution becomes 'chaotic'.

For small k , $\Gamma_k = -i v k$,
 $v^2 = \frac{n}{\varepsilon+p} (\frac{\partial p}{\partial n})_S$ or $v^2 = \frac{n}{\varepsilon+p} (\frac{\partial p}{\partial n})_T < 0$

Relativistic heavy-ion collisions

(6)



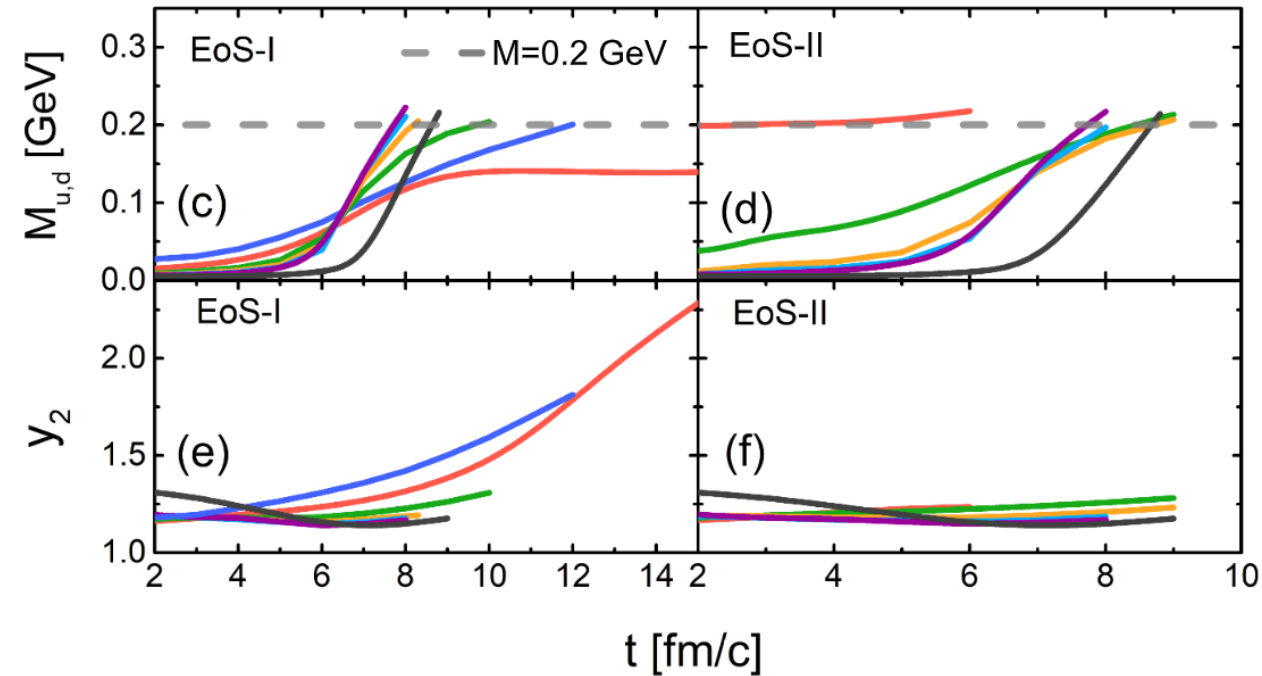
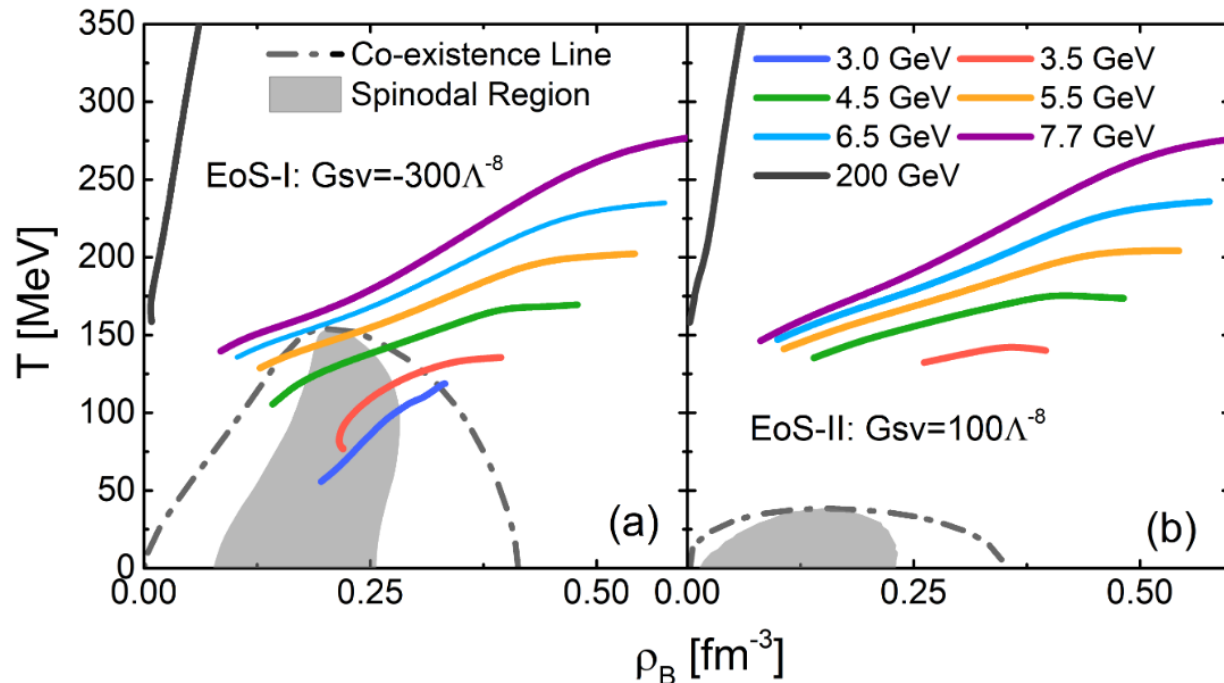
Trajectories in the phase diagram

(7)

Phase trajectories of central cells in the phase diagram

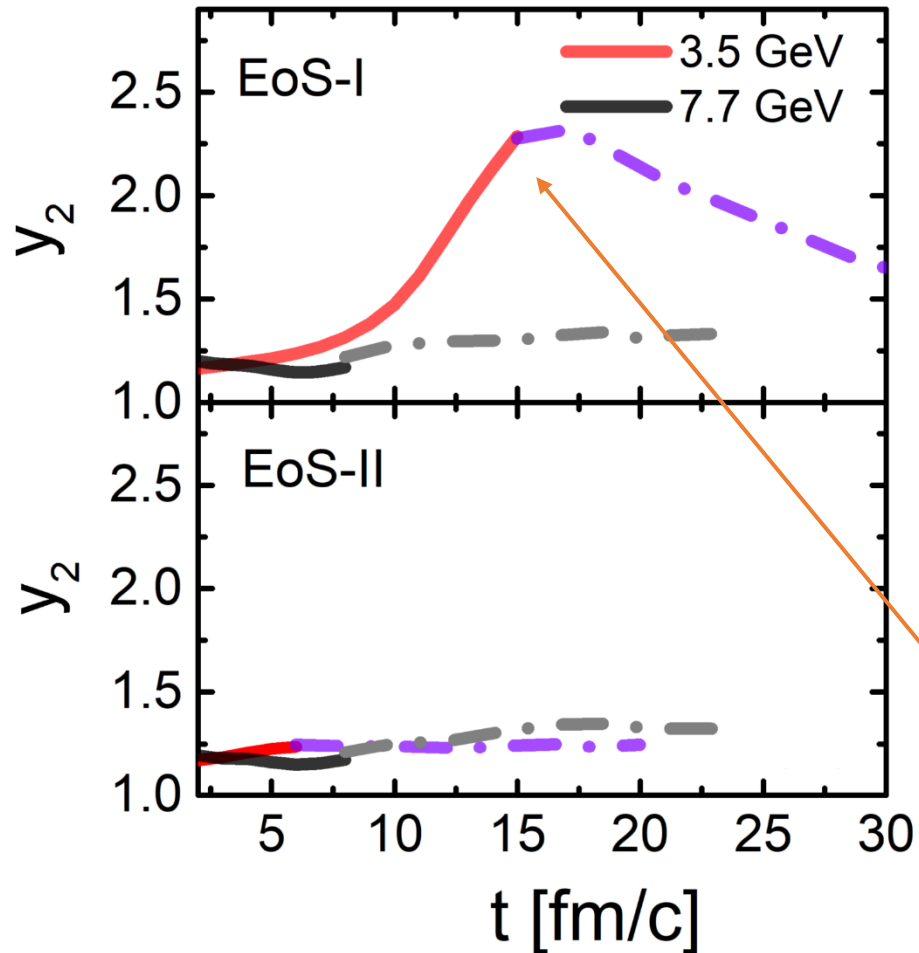
$$\overline{\rho^N} = \frac{\int d\mathbf{x} \rho^{(N+1)}(\mathbf{x})}{\int d\mathbf{x} \rho(\mathbf{x})}$$

$$y_2 = \frac{[\int d\mathbf{x} \rho(\mathbf{x})][\int d\mathbf{x} \rho^3(\mathbf{x})]}{[\int d\mathbf{x} \rho^2(\mathbf{x})]^2}$$



Survival of density fluctuation in an expanding fireball (8)

Off-equilibrium effects



Density moment:

$$\overline{\rho^N} = \frac{\int d\mathbf{x} \rho^{(N+1)}(\mathbf{x})}{\int d\mathbf{x} \rho(\mathbf{x})}$$

$$y_2 = \frac{[\int d\mathbf{x} \rho(\mathbf{x})][\int d\mathbf{x} \rho^3(\mathbf{x})]}{[\int d\mathbf{x} \rho^2(\mathbf{x})]^2}$$

If the expansion is self-similar or scale invariant

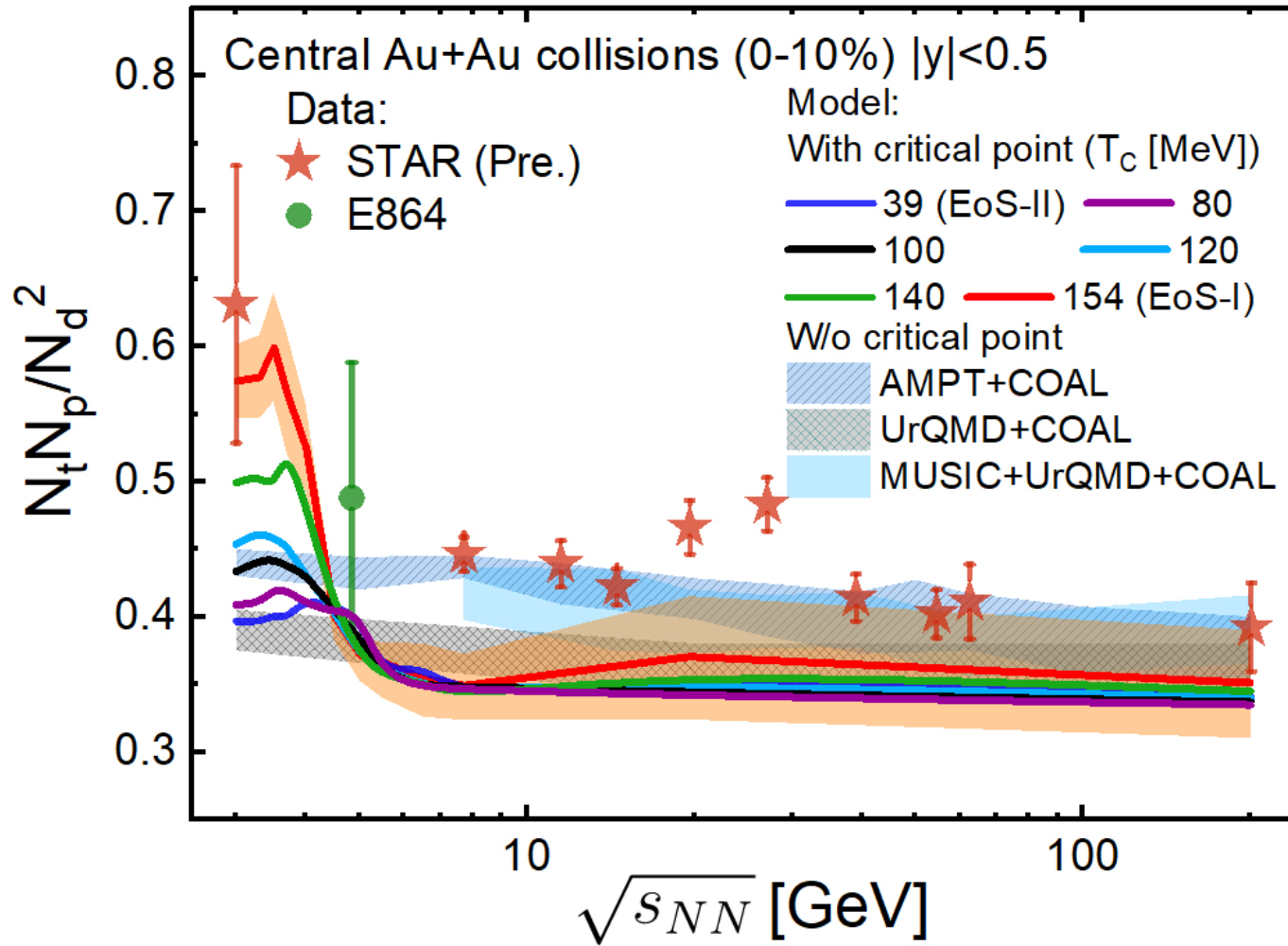
$$\rho(\lambda(t)x, t) = \alpha(t)\rho(x, t_h)$$

then $y_2(t) = y_2(t_h)$, i.e., remains a constant

3. Spinodal enhancement of $N_t N_p / N_d^2$

Collision energy dependence

(9)



1. Without a critical point:
The energy dependence of tp/d^2 is almost flat.
2. With a first-order phase transition:
The spinodal instability induced enhancement of tp/d^2 during the first-order phase transition increases as increasing the critical temperature.

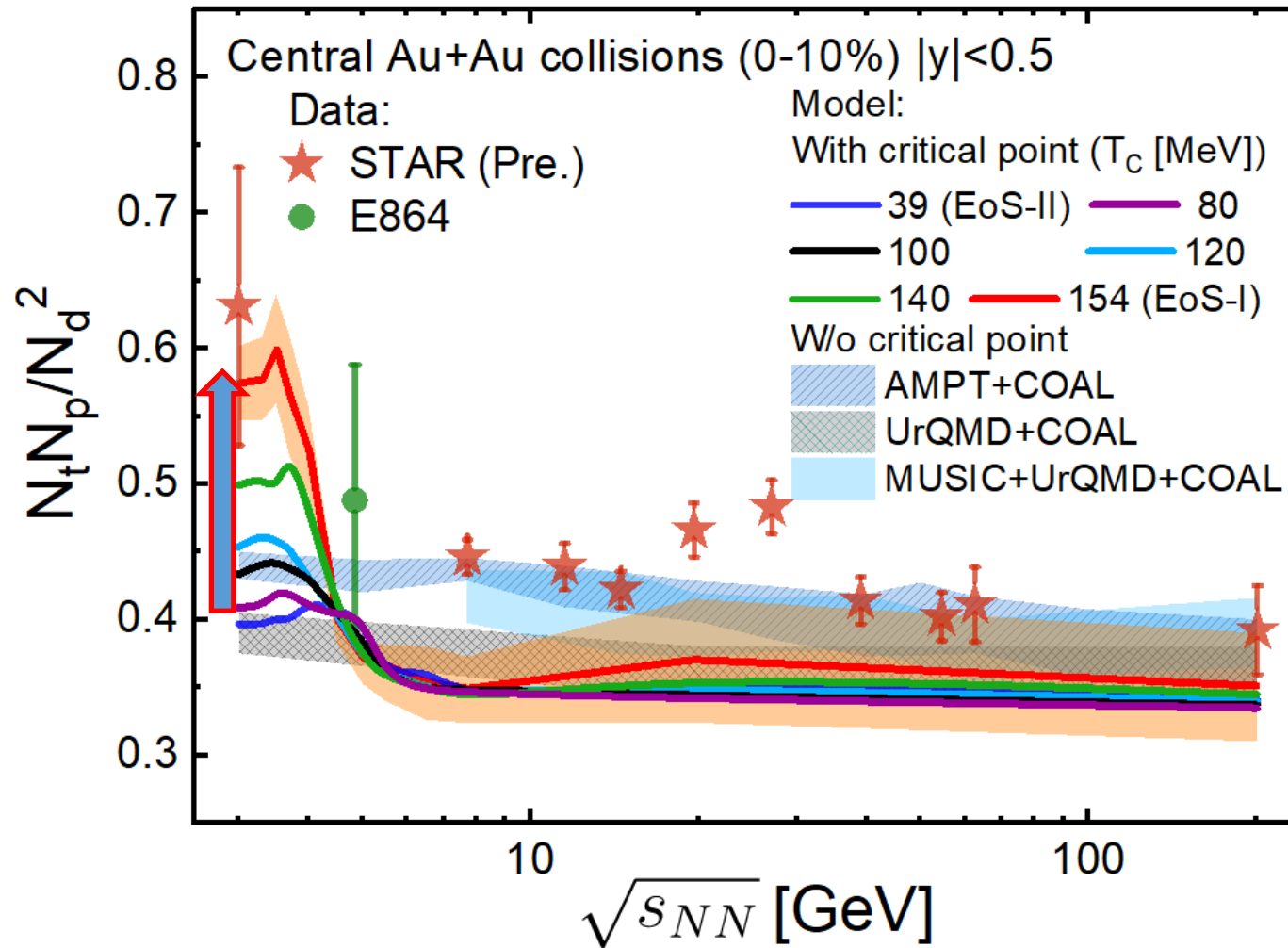
STAR, PRL130, 202302 (2023)

Hui Liu (STAR), QM2022

T. A. Armstrong et al. (E864), Phys. Rev. C 61, 064908 (2000).

Collision energy dependence

(10)



1. Without a critical point:
The energy dependence of tp/d^2 is almost flat.
2. With a first-order phase transition:
The spinodal instability induced enhancement of tp/d^2 during the first-order phase transition increases as increasing the critical temperature.

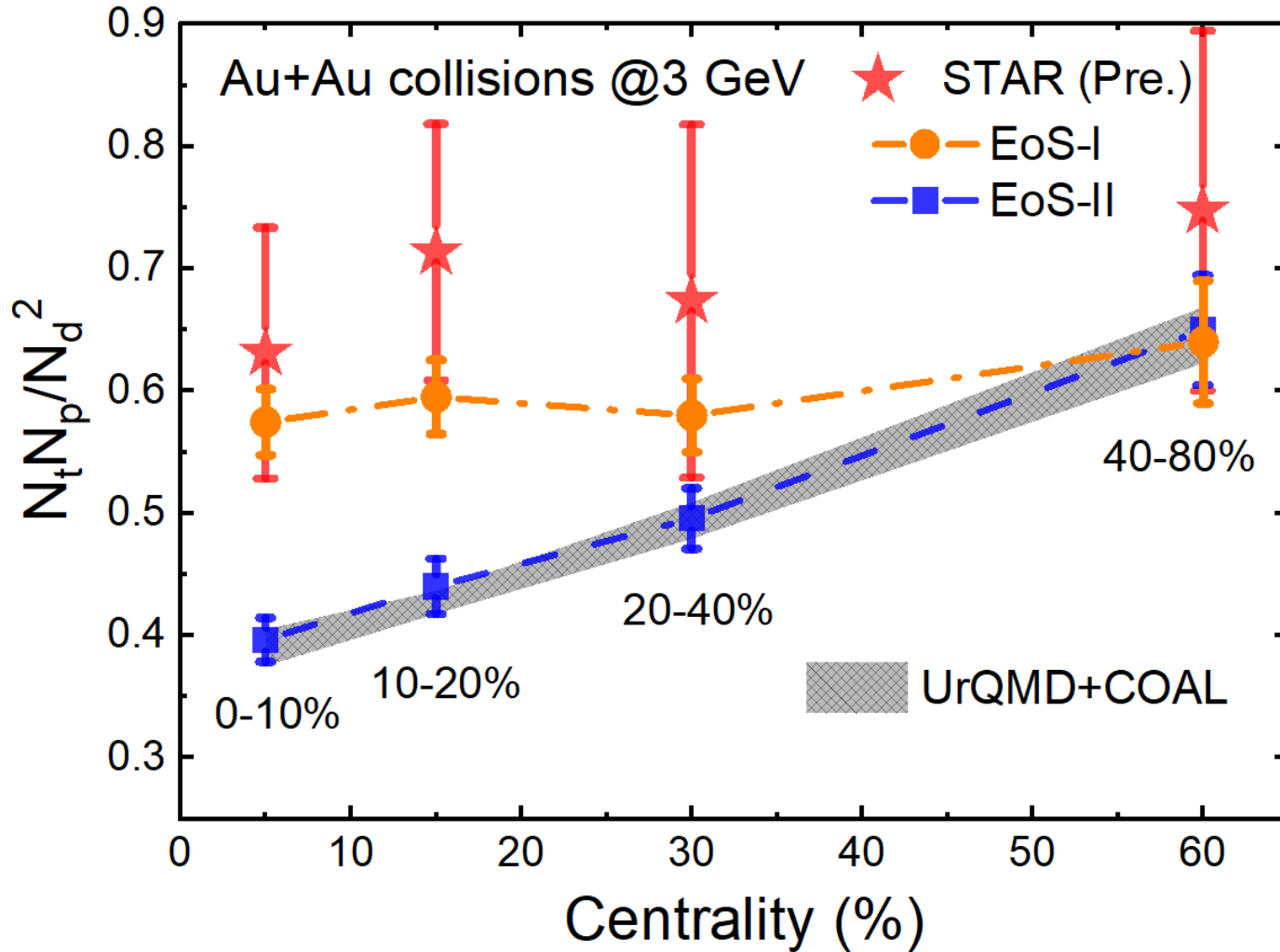
STAR, PRL130, 202302 (2023)

Hui Liu (STAR), QM2022

T. A. Armstrong et al. (E864), Phys. Rev. C 61, 064908 (2000).

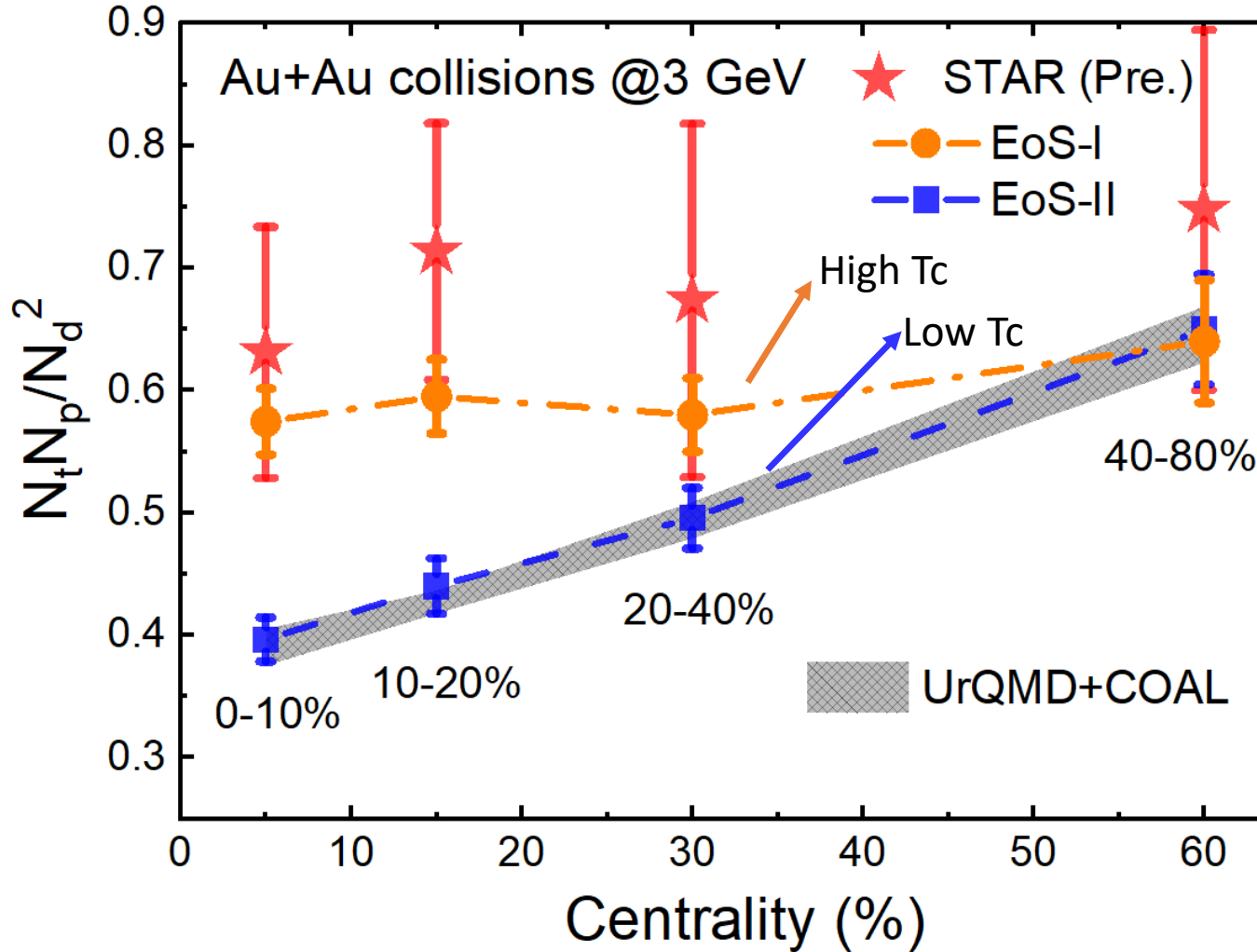
Centrality dependence

(11)



Centrality dependence

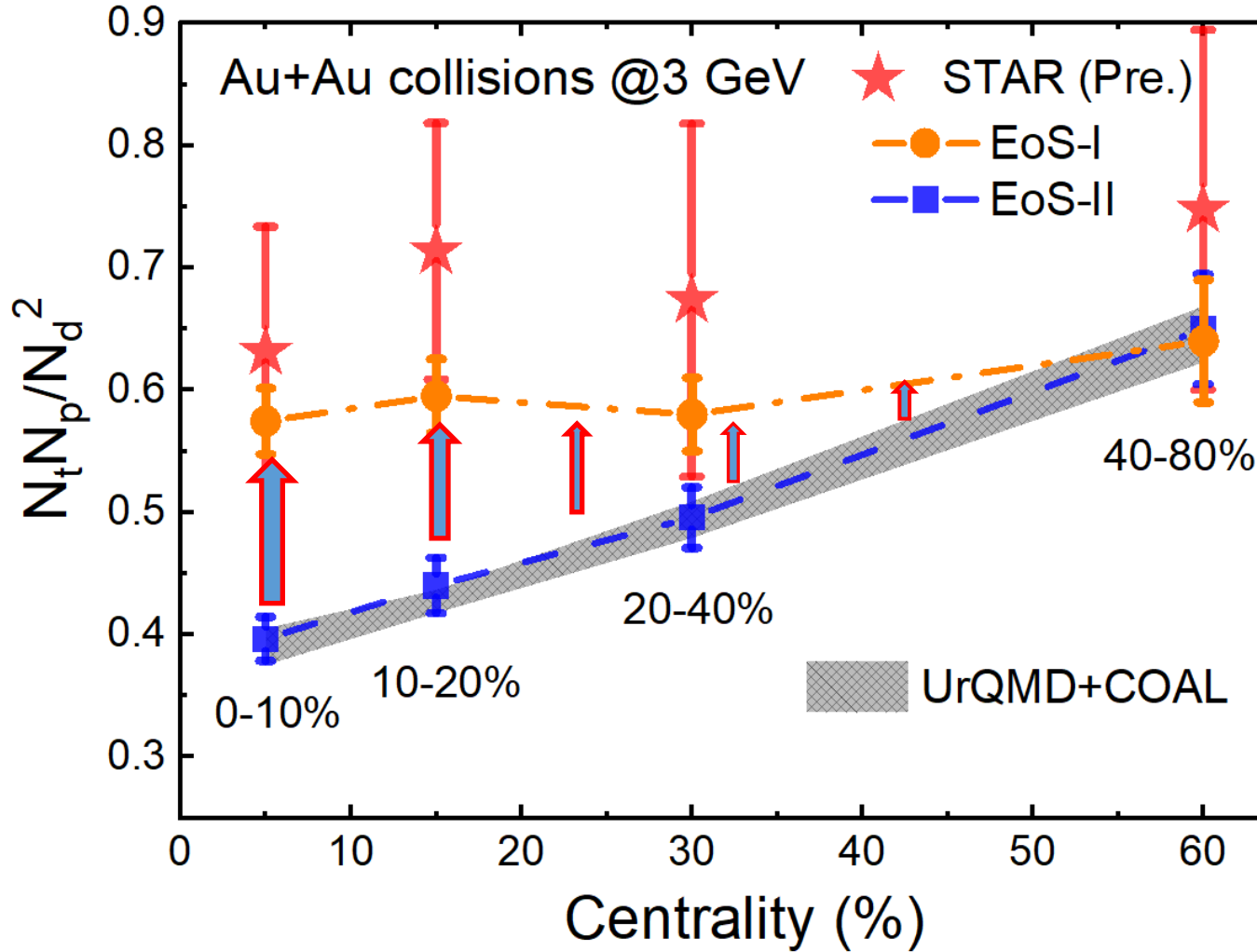
(12)



The spinodal enhancement of tp/d^2 subsides with increasing collision centrality because of smaller fireball lifetime in more peripheral collisions.

Centrality dependence

(13)



The spinodal enhancement of tp/d^2 subsides with increasing collision centrality because of smaller fireball lifetime in more peripheral collisions.

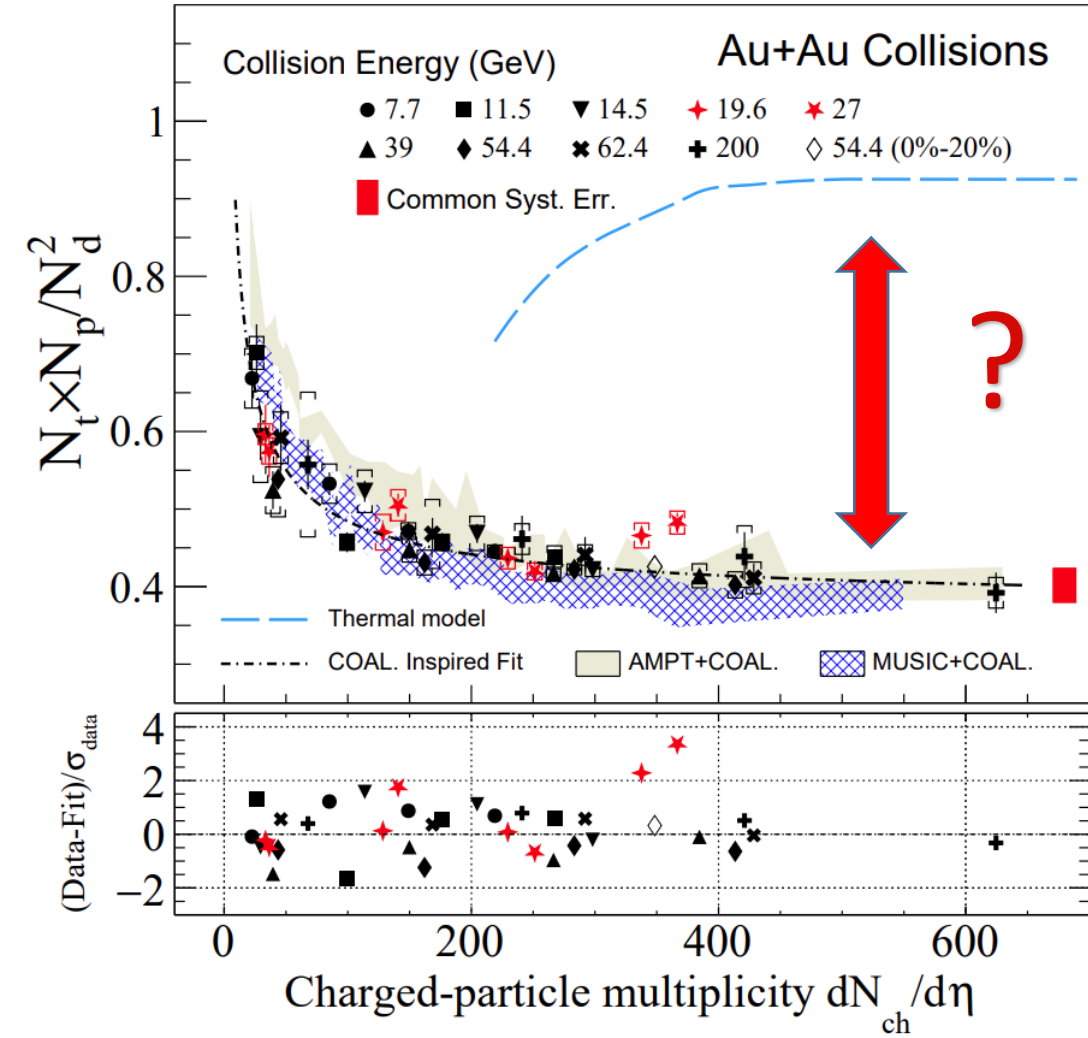
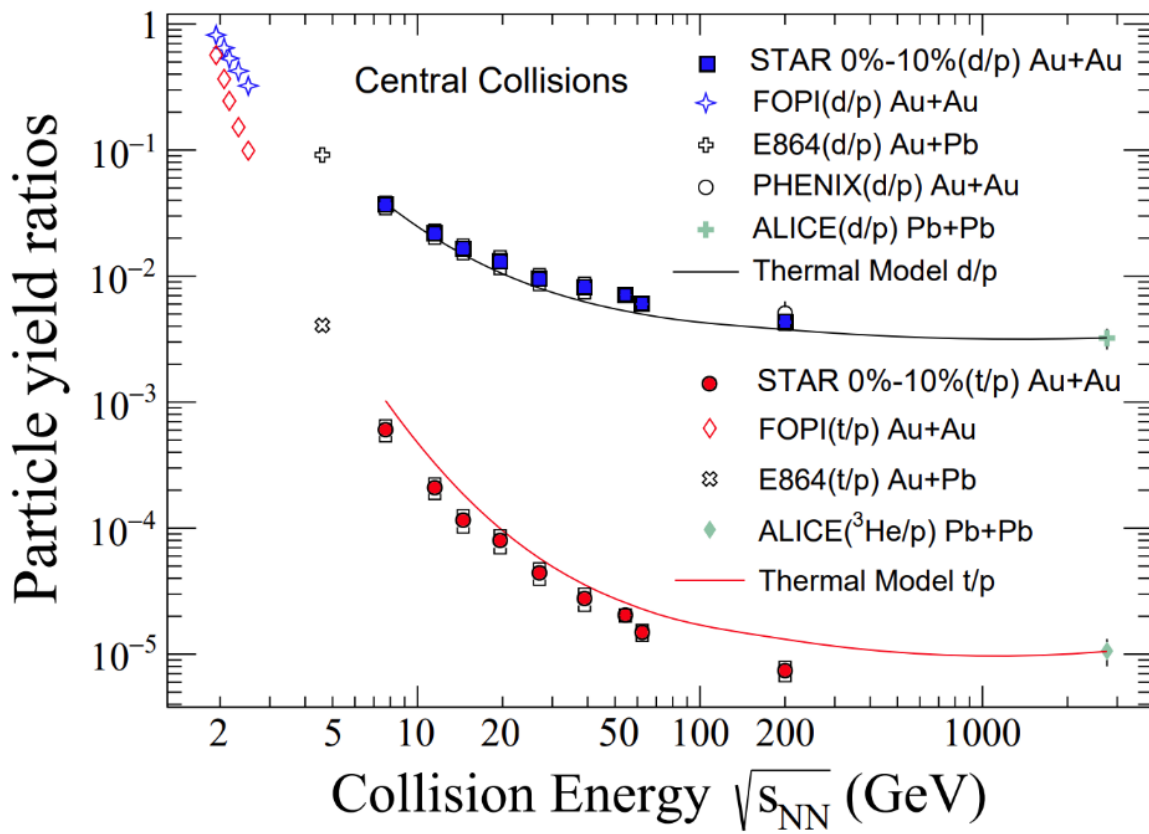
The slope with EoS-I is 5 times smaller

4. The triton ‘puzzle’ and its solution

The Triton ‘Puzzle’ at RHIC

(14)

STAR, Phys.Rev.Lett. 130 (2023) 202301

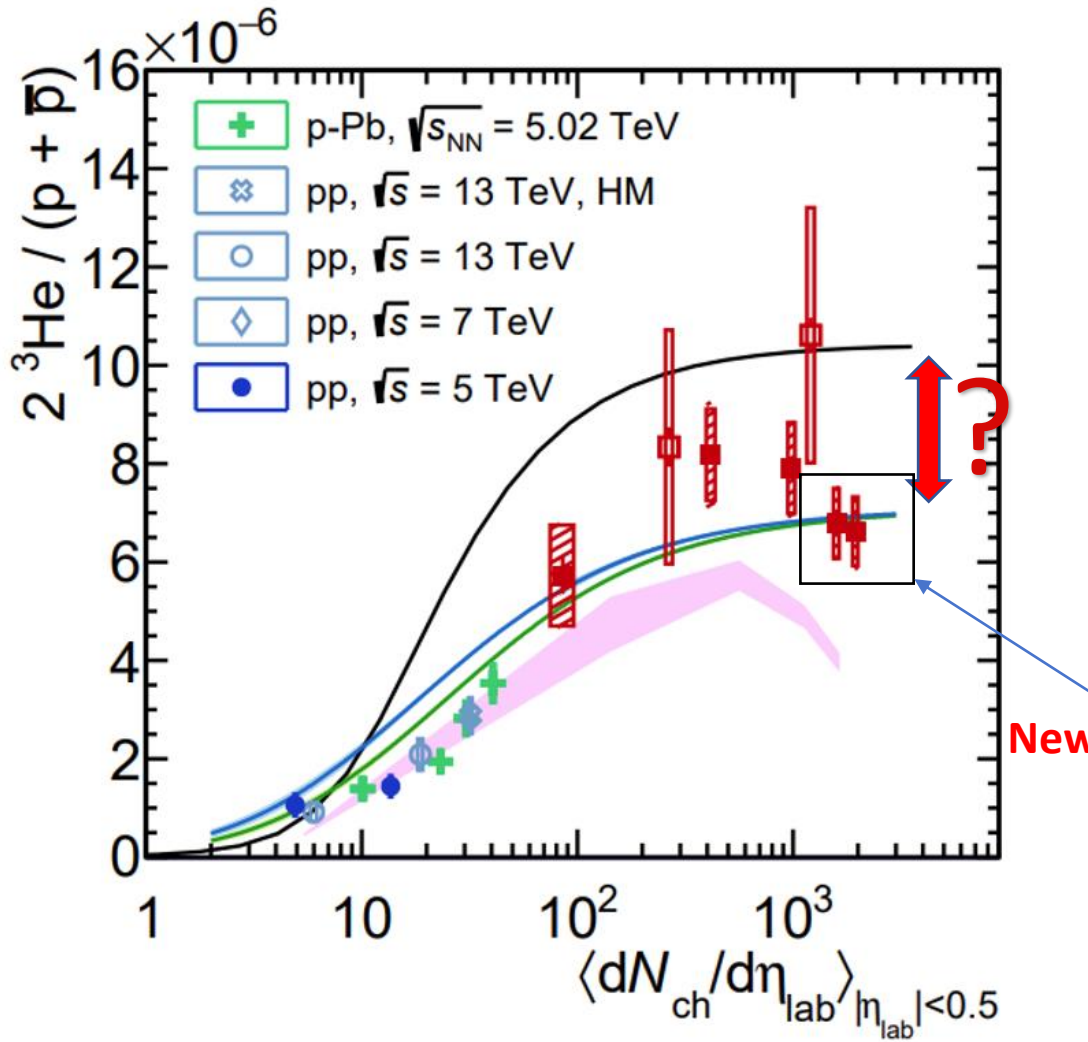


Triton yields at RHIC are overestimated by the statistical hadronization model.

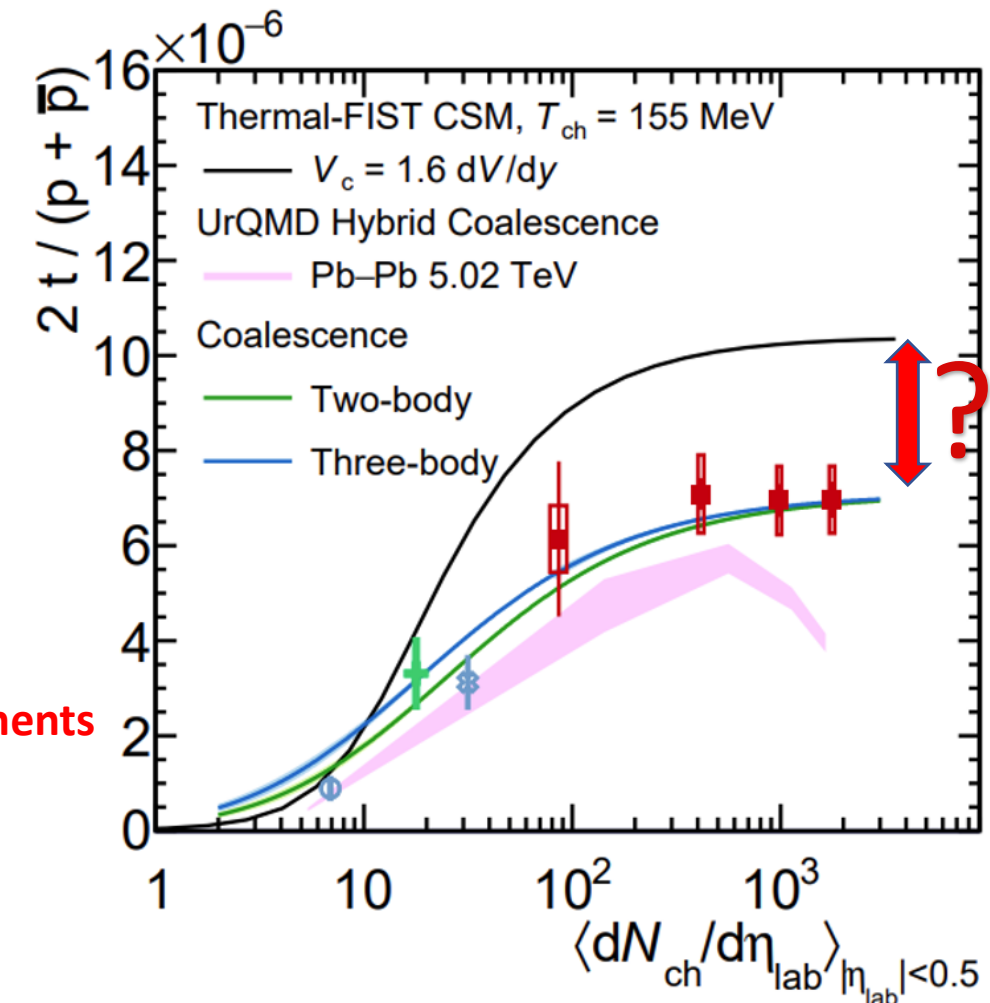
The Triton ‘Puzzle’ at LHC

(15)

ALICE, Phys. Rev. C 107, 064904 (2023)



New measurements

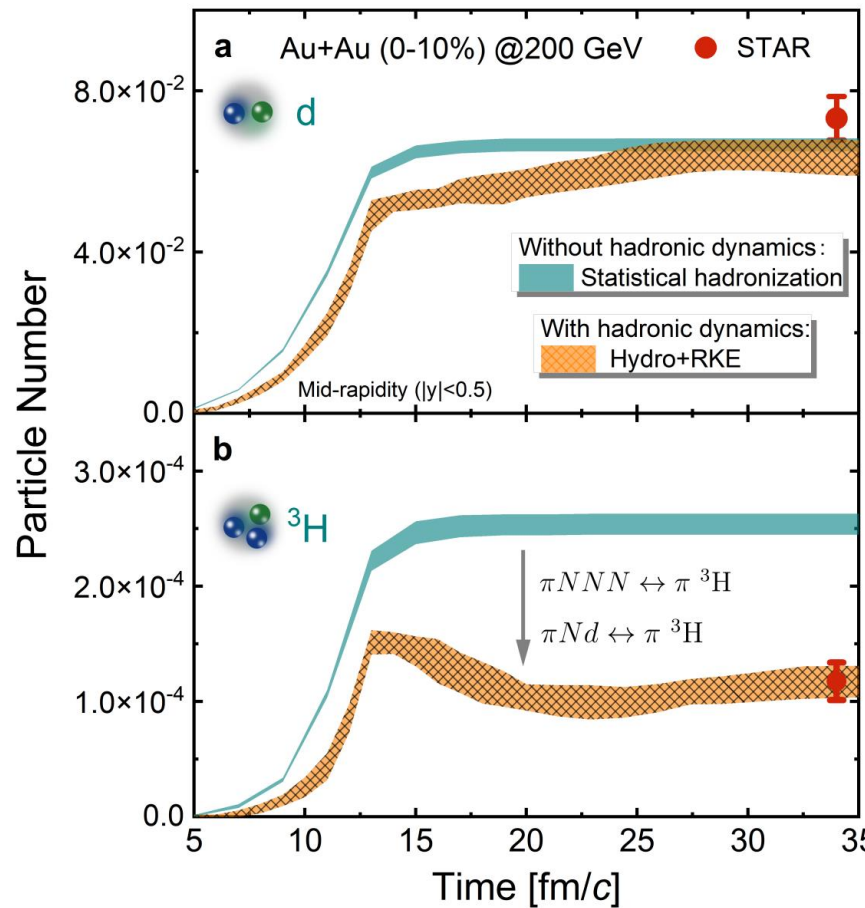


Triton (helium-3) yields at LHC are overestimated by the statistical hadronization model.

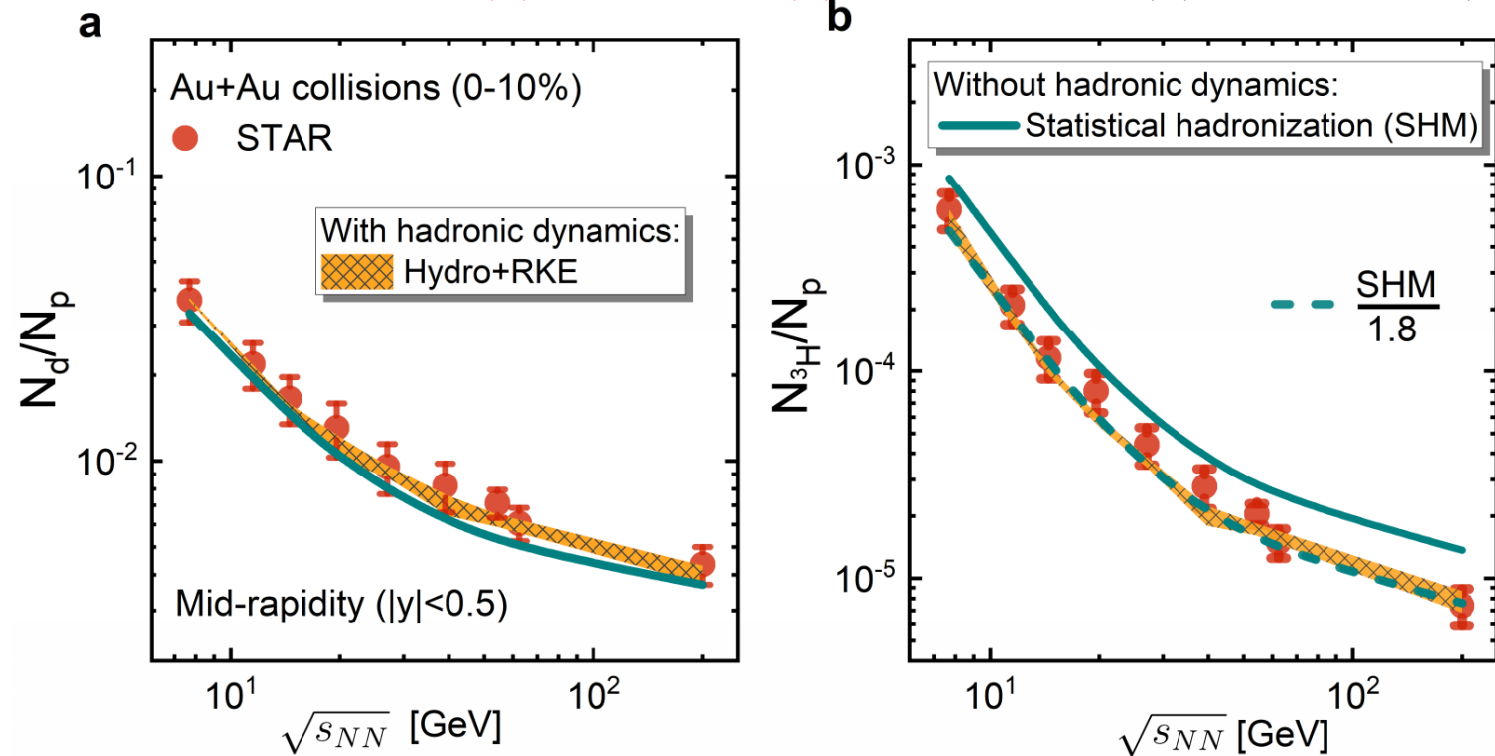
Solution: Hadronic re-scatterings

(16)

K. J. Sun, R. Wang, C. M. Ko, Y. G. Ma, and C. Shen, 2207.12532(2022) Data from STAR, PRL 130, 202301 (2023)



- A = 2 $\pi NN \leftrightarrow \pi d, NNN \leftrightarrow Nd$
- A = 3 $\pi NNN \leftrightarrow \pi t(h), \pi Nd \leftrightarrow \pi t(h), NNNN \leftrightarrow Nt(h), NNd \leftrightarrow Nt(h)$



Hadronic re-scatterings have small effects on the final deuteron yields (see also D. Oliinychenko et al. PRC 99, 044907 (2019)), but they reduce the triton yields by about a factor of 1.8. Similar strong hadronic effects occur at the LHC energies.

Main findings:

1. Using a novel transport model, we find that large density inhomogeneities generated by the **spinodal instability** during the first-order QCD phase transition can survive the fast expansion of the subsequent hadronic matter expansion and lead to an enhanced $N_t N_p / N_d^2$ in central Au+Au collisions at $\sqrt{s_{NN}} = 3 - 5$ GeV for $T_c \geq 80$ MeV, which is in accordance with the STAR measurements.
2. **Hadronic re-scatterings** are found to reduce the triton yields by about a factor of 2 during the post-hadronization stage, which resolves the overestimation of SHM on the triton production at both RHIC and LHC energies. (Hadronic re-scatterings also play an important role in explaining the production of hadronic resonances like K^* , $\Lambda(1520)$, and etc. [see talk by Sonali Padhan for ALICE])

Backup

Why $N_t N_p / N_d^2$? (1)

Density matrix formulation
Phase-space representation:

$$N_d = \frac{3}{4} \int d\Gamma f_{pn}(\vec{p}_1, \vec{r}_1, \vec{p}_2, \vec{r}_2) \times W_d(\vec{r}, \vec{p})$$

$$W_d(\vec{r}, \vec{p}) = \frac{1}{\pi\hbar} \int d\vec{r}' \psi_d^*(\vec{r} + \vec{r}') \psi_d(\vec{r} - \vec{r}') e^{2i\vec{p}\cdot\vec{r}'}$$

Wigner function(Gaussian):

$$W_d(r, k) = 8 \exp\left(-\frac{r^2}{\sigma_d^2} - \sigma_d^2 p^2\right) \quad \sigma_d \approx 2.26 \text{ fm}$$

with density fluctuation and correlation:

$$f_{np}(x_1, p_1; x_2, p_2) = \rho_{np}(x_1, x_2)(2\pi mT)^{-3} e^{-\frac{p_1^2 + p_2^2}{2mT}}$$

$$\rho_{np}(x_1, x_2) = \rho_n(x_1)\rho_p(x_2) + C_2(x_1, x_2)$$

$$\rho_n(x) = \langle \rho_n \rangle + \delta\rho_n(x) \quad \rho_p(x) = \langle \rho_p \rangle + \delta\rho_p(x)$$

$\delta\rho(x)$ denotes density fluctuation over space or inhomogeneity,

$C_{np} = \langle \delta\rho_n(x)\delta\rho_p(x) \rangle / (\langle \rho_n \rangle \langle \rho_p \rangle)$	$\langle \dots \rangle \equiv \frac{1}{V} \int dx$
$\Delta\rho_n = \langle \delta\rho_n(x)^2 \rangle / \langle \rho_n \rangle^2$	

$$C_2(x_1 - x_2) \approx \lambda \langle \rho_n \rangle \langle \rho_p \rangle \frac{e^{-|x_1 - x_2|/\xi}}{|x_1 - x_2|^{1+\eta}} \quad (\text{singular part only})$$

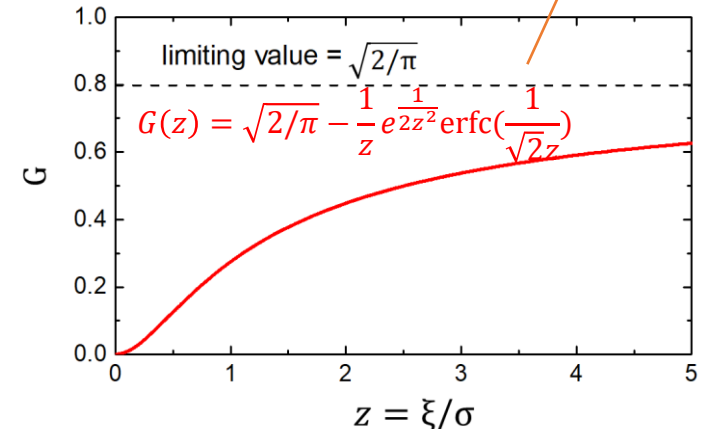
with ξ being the density-density correlation length
 $0 < \langle \delta N^2 \rangle \sim \int dx C_2(x) \sim \lambda \xi^2 \rightarrow \lambda > 0$

$$N_d \propto \text{Tr}[\hat{\rho}_s \hat{\rho}_d]$$

Phys. Lett. B 774, 103 (2017); 781, 499 (2018); 816, 136258 (2021)

Encodes many-body density fluctuation/correlation

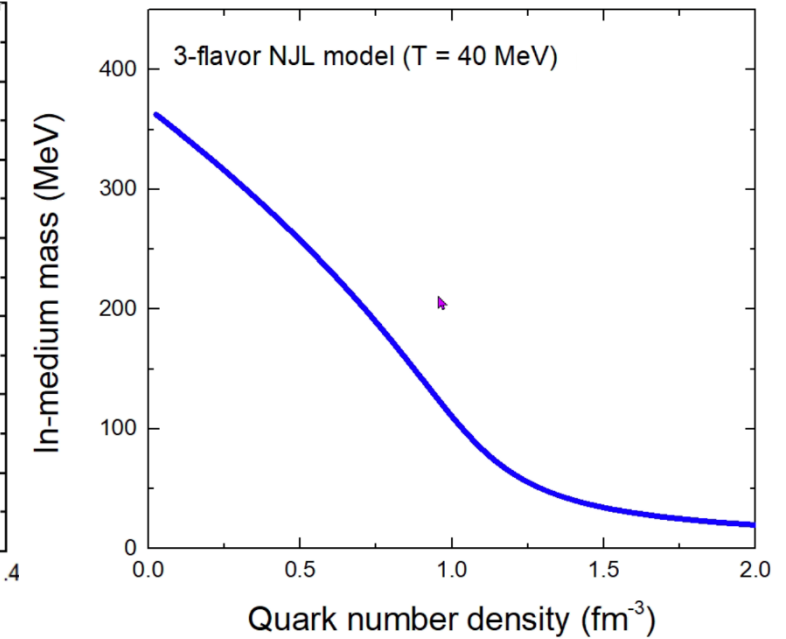
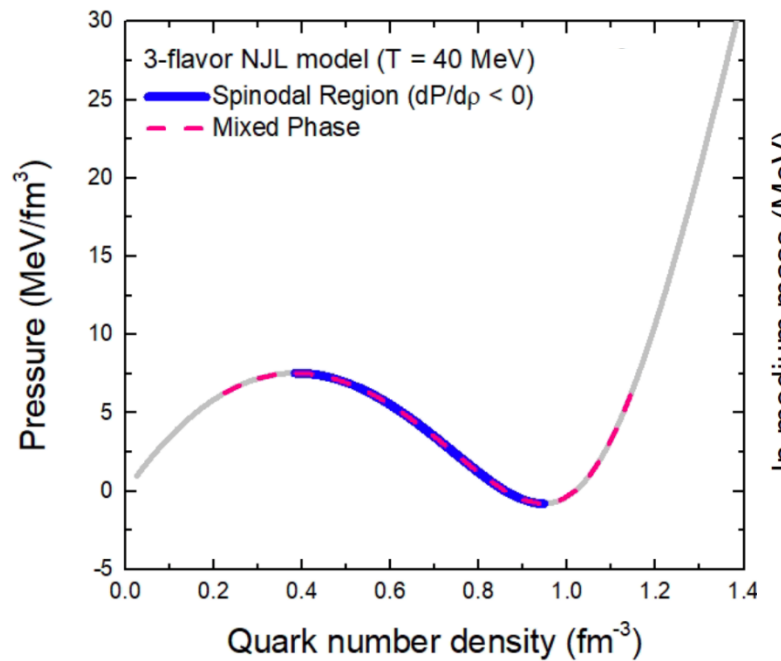
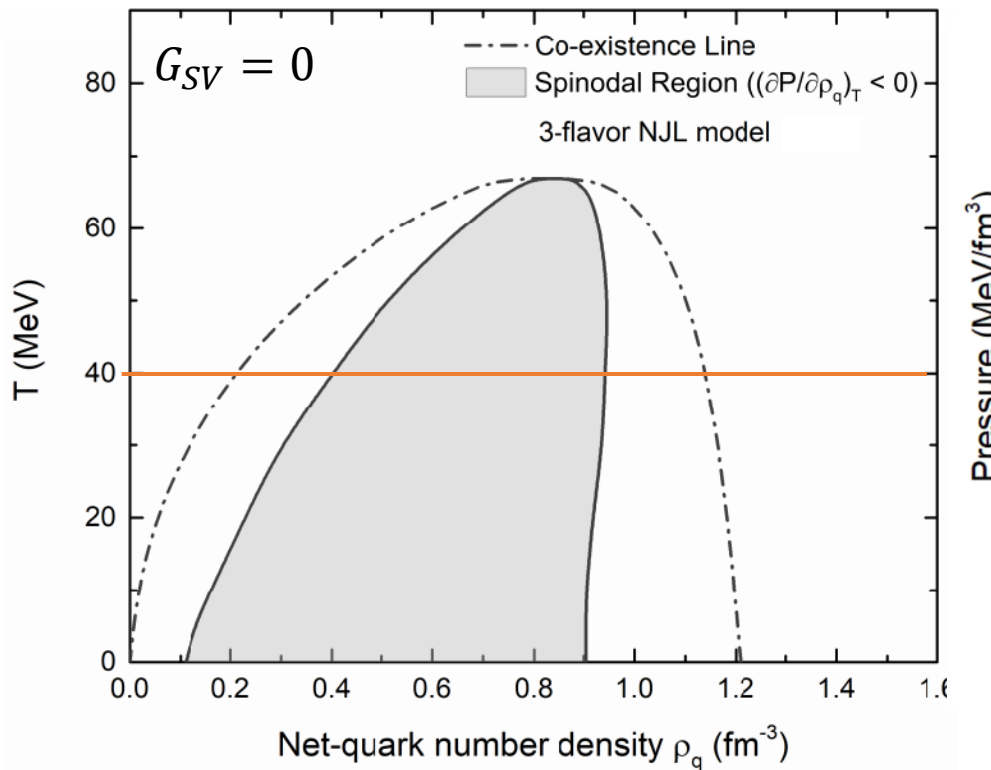
$$\begin{aligned} N_d &\approx \frac{3}{\sqrt{2}} \left(\frac{2\pi}{mT}\right)^{\frac{3}{2}} N_p \langle \rho_n \rangle [1 + C_{np} + \frac{\lambda}{\sigma_d} G\left(\frac{\xi}{\sigma_d}\right)] \\ N_t &= \frac{3^{3/2}}{4} \left(\frac{2\pi}{mT}\right)^3 N_p \langle \rho_n \rangle^2 [1 + 2C_{np} + \Delta\rho_n + \frac{3\lambda}{\sigma_t} G\left(\frac{\xi}{\sigma_t}\right) + O(G^2)] \end{aligned}$$



Ratio: $\frac{N_t N_p}{N_d^2} \approx \frac{1}{2\sqrt{3}} \left[1 + \Delta\rho_n + \frac{\lambda}{\sigma} G\left(\frac{\xi}{\sigma}\right) \right]$

In-medium quark mass

(2)



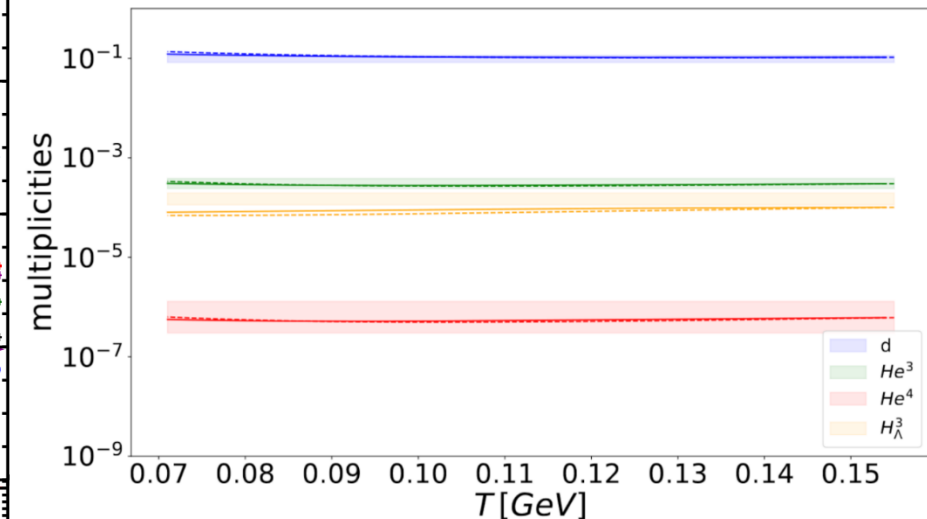
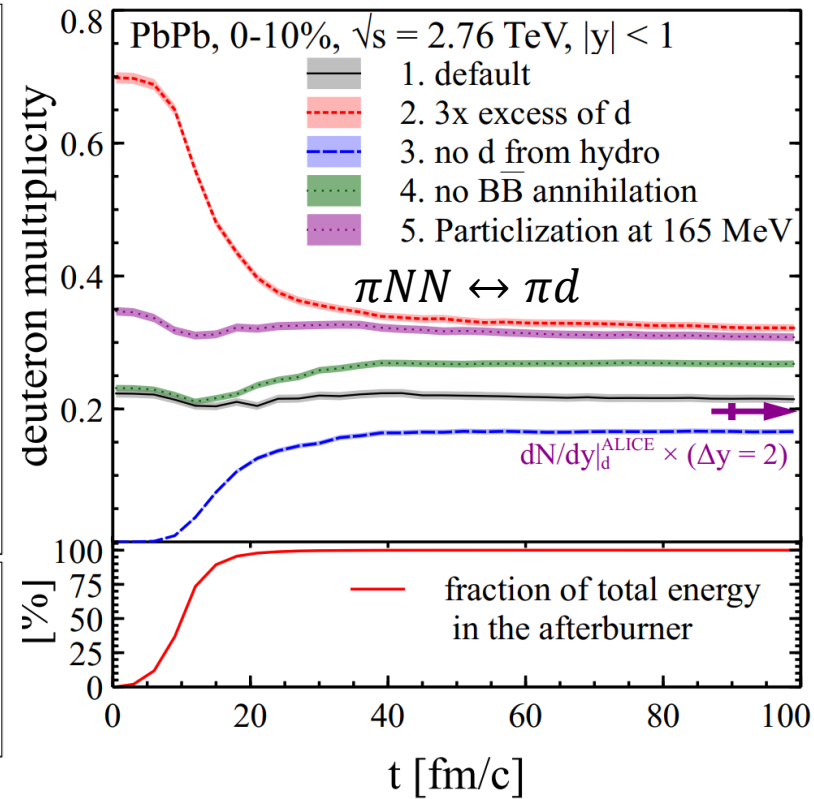
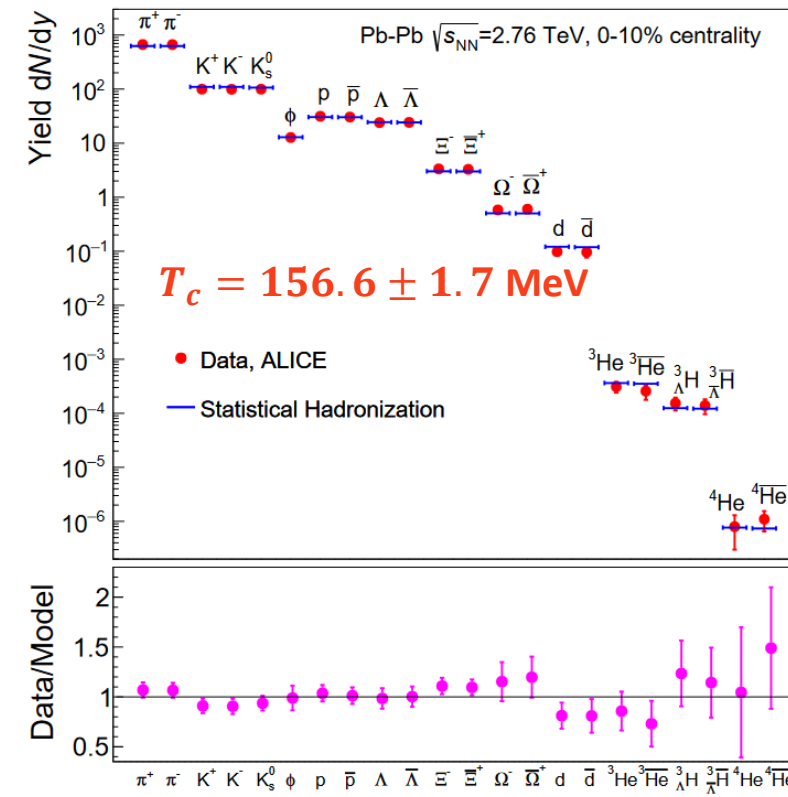
The Triton ‘Puzzle’

Earlier theoretical results

D. Oliinychenko, et al., PRC99, 044907 (2019)

V. Vovchenko, et al., PLB800, 135131 (2020)

T. Neidig, et al., PLB827, 136891 (2022)



The obtained hadronic effects on light nuclei production are small!

A. Andronic, P. Braun-Munzinger, J. Stachel, H. Stöcker, PLB 697, 203 (2011)

A. Andronic, P. Braun-Munzinger, K. Redlich, J. Stachel, Nature 561, 321 (2018)

Relativistic Kinetic Approach to the Little-Bang Nucleosynthesis (4)

K. J. Sun, R. Wang, C. M. Ko, Y. G. Ma, and C. Shen, 2207.12532(2022)

Relativistic kinetic equation for $\pi NN \leftrightarrow \pi d$

$$\frac{\partial f_d}{\partial t} + \frac{\mathbf{P}}{E_d} \cdot \frac{\partial f_d}{\partial \mathbf{R}} = -\mathcal{K}^> f_d + \mathcal{K}^<(1 + f_d)$$

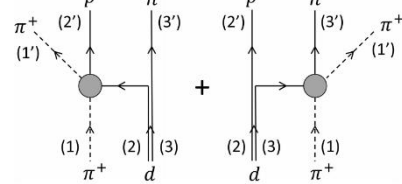
with collision integral:

$$\begin{aligned} \text{R.H.S.} = & \frac{1}{2g_d E_d} \int \prod_{i=1'}^{3'} \frac{d^3 \mathbf{p}_i}{(2\pi)^3 2E_i} \frac{d^3 \mathbf{p}_\pi}{(2\pi)^3 2E_\pi} \frac{E_d d^3 \mathbf{r}}{m_d} \\ & \times 2m_d W_d(\tilde{\mathbf{r}}, \tilde{\mathbf{p}}) (\overline{|\mathcal{M}_{\pi^+ n \rightarrow \pi^+ n}|^2} + n \leftrightarrow p) \\ & \times \left[- \left(\prod_{i=1'}^{3'} (1 \pm f_i) \right) g_\pi f_\pi g_d f_d + \frac{3}{4} \left(\prod_{i=1'}^{3'} g_i f_i \right) \right. \\ & \quad \left. \times (1 + f_\pi)(1 + f_d) \right] \times (2\pi)^4 \delta^4(p_{\text{in}} - p_{\text{out}}) \end{aligned}$$

Nonlocal collision integral to take into account the effects of finite nuclei sizes. W_d denotes deuteron Wigner function.

P. Danielewicz et al., NPA533, 712 (1991); PLB274, 268 (1992); Annals of Physics 152, 239(1984);

Impulse approximation (IA): Length/energy scale:



$$\lambda_{\text{thermal}} \sim 0.5 \text{ fm} \ll r_{np} \sim 4 \text{ fm}$$

FIG. 1. Diagrams for the reaction $\pi^+ d \leftrightarrow \pi^+ np$ in the impulse approximation. The filled bubble indicates the intermediate states such as a Δ resonance.

Solving kinetic equations with the stochastic method using test particles

Probability for reaction $\pi d \leftrightarrow \pi NN$ to take place in volume ΔV and time interval Δt are given by

$$\begin{aligned} P_{23}|_{\text{IA}} &\approx F_d v_{\pi^+ p} \sigma_{\pi^+ p \rightarrow \pi^+ p} \frac{\Delta t}{N_{\text{test}} \Delta V} + (p \leftrightarrow n), \\ P_{32}|_{\text{IA}} &\approx \frac{3}{4} F_d v_{\pi^+ p} \sigma_{\pi^+ p \rightarrow \pi^+ p} \frac{\Delta t W_d}{N_{\text{test}}^2 \Delta V} + (p \leftrightarrow n) \end{aligned}$$

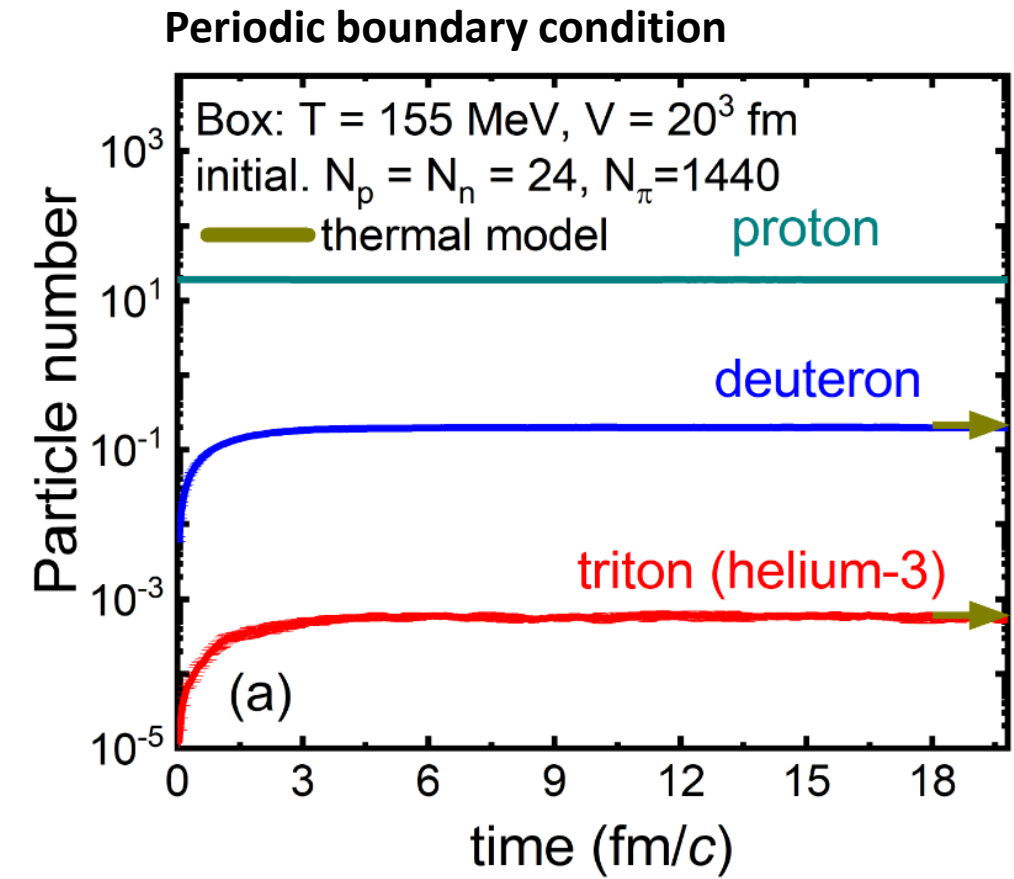
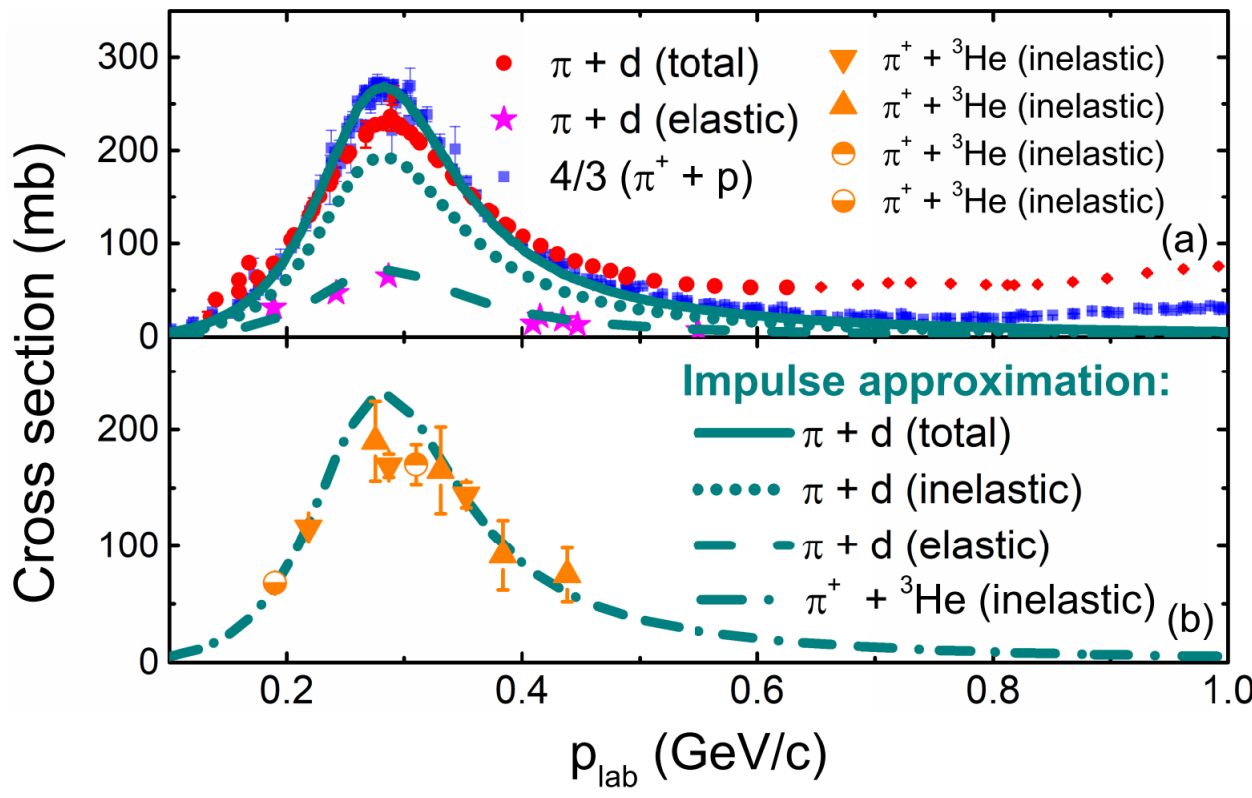
For triton or helium-3:

$$P_{42}|_{\text{IA}} \approx \frac{1}{4} F_t \frac{v_{\pi N} \sigma_{\pi N \rightarrow \pi N} \Delta t}{N_{\text{test}}^3 \Delta V} W_t$$

'renormalization' factor F_d, F_t which can be fixed by πd and πt cross sections.

Thermal Limit

(5)



Relativistic Kinetic Approach versus Coalescence

(6)

Coalescence and flow in ultra-relativistic heavy ion collisions

Rüdiger Scheibl and Ulrich Heinz

Institut für Theoretische Physik, Universität Regensburg, D-93040 Regensburg, Germany

(March 16, 1999 — published in Physical Review C 59 (1999), 1585-1602)

$$\begin{aligned} \frac{dN_d}{d^3P_d} = & \frac{-3i}{(2\pi)^3} \int d^4r_d d^3r \int \frac{d^4p_1}{(2\pi)^4} \frac{d^3p_2}{(2\pi)^3} \\ & \times (2\pi)^4 \delta^4(P_d - p_1^* - p_2) \mathcal{D}\left(\mathbf{r}, \frac{\mathbf{p}_1 - \mathbf{p}_2}{2}\right) \\ & \times \left(\Sigma_p^<(p_1^*, r_+) f_n^W(p_2, r_-) + \Sigma_n^<(p_1^*, r_+) f_p^W(p_2, r_-) \right), \end{aligned} \quad (3.12)$$

$$\begin{aligned} -i\Sigma_N^<(p^*, x) = & \sum_j \int \frac{d^3q}{(2\pi)^3} \frac{d^3p'}{(2\pi)^3} \frac{d^3q'}{(2\pi)^3} \\ & \times (2\pi)^4 \delta^4(p^* + q - p' - q') |M_{Nj \rightarrow Nj}|^2 \\ & \times f_N^W(p', x) f_j^W(q', x) (1 \pm f_j^W(q, x)). \end{aligned} \quad (3.13)$$

$$-i\Sigma_N^<(p^*, x) = \frac{f_N(p^*, x)}{\tau_{\text{sca}}^N(\mathbf{p}, x)}. \quad (3.16)$$



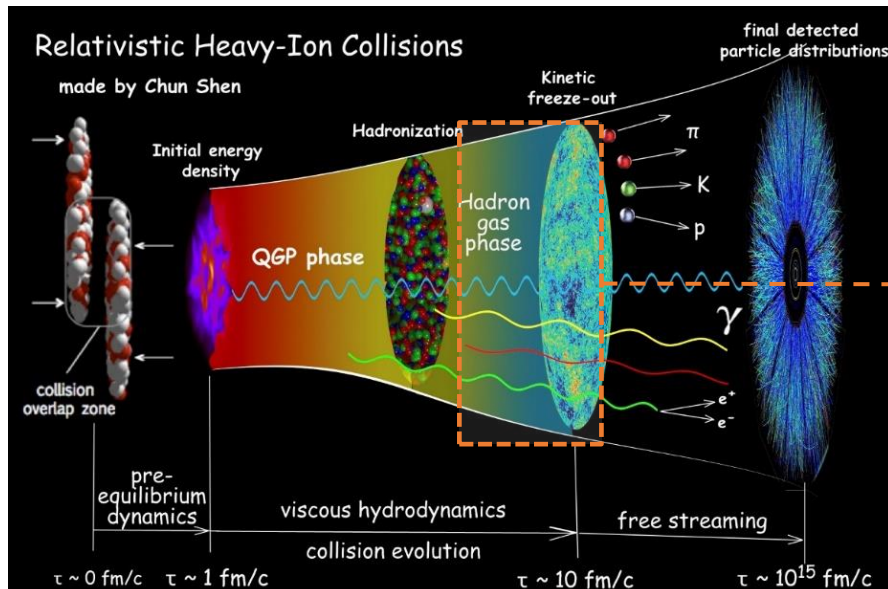
$$\begin{aligned} \frac{dN_d}{d^3P_d} = & \frac{3}{(2\pi)^3} \int d^3r_d \int \frac{d^3r}{(2\pi)^3} \frac{d^3q}{(2\pi)^3} \mathcal{D}(\mathbf{r}, \mathbf{q}) \\ & \times f_p(q_+, r_+) f_n(q_-^*; r_-). \end{aligned} \quad (3.17)$$

Final-state coalescence

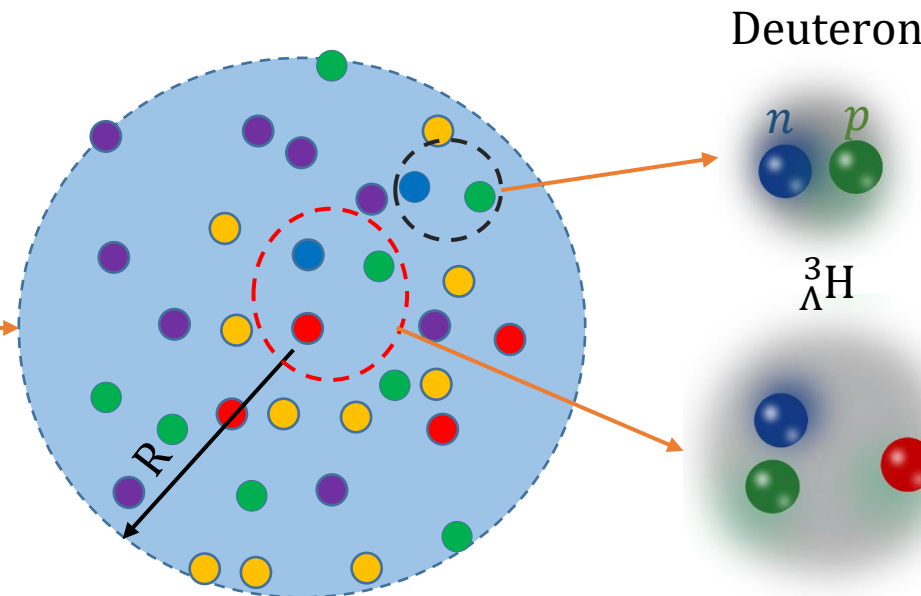
(7)

R. Scheibl and U. W. Heinz, PRC59. 1585(1999);

R. Scheibl and U. W. Heinz, PRC59. 1585(1999)



Coalescence Model



Density Matrix Formulation
(sudden approximation)

$$N_A = \text{Tr}(\hat{\rho}_s \hat{\rho}_A) \\ = g_c \int d\Gamma \rho_s(\{x_i, p_i\}) \times W_A(\{x_i, p_i\})$$

Wigner function of light cluster

Overlap between source distribution function and Wigner function of light nuclei